A Live Imaging Characterization of Early Nephric Duct Development in Mice

Michael Marcotte
Department of Biochemistry, McGill University, Montreal
August 2016

A thesis submitted to McGill University in partial fulfillment of the requirements of the degree of Master of Science.

Table of Contents

List of Figures

List of Tables

Acknowledgements

I must first acknowledge Dr. Maxime Bouchard for his guidance, mentorship, support and patience. I would also like to acknowledge past and present members of the Bouchard lab for advice, assistance and instruction. I would especially like to acknowledge Dr. David Grote for establishing the project and developing the initial protocol for live imaging. I must also acknowledge my supervisory committee members Dr. Yojiro Yamanaka, Dr. Thomas Duchaine and Dr. Philippe Gros. Finally I acknowledge Carmina Angelica Perez Romero for continued support, advice and encouragement.

Preface

This thesis includes two figures that were made in collaboration. Notably panels A, B, E and F of figure 8 and panels B, D and F of figure 9 were provided by our collaborators Ian Chia and Ekaterina Batourina from Dr. Cathy Mendelsohn's lab. I provided the remaining panels in these figures. Supplementary videos can be found at the following website:
https://www.dropbox.com/sh/kydd5x2gvb7udr6/AABKwneSUXK6GjkkK-s7qk90a?dl=0

Abstract

Congenital abnormalities of the kidney and urinary tract are among the most common birth defects. A potential cause of such defects is the failure of the nephric duct to extend to reach the cloaca. Better understanding of the process will be useful, in treatment, diagnosis and prevention of disease. We have established conditions suitable for the live image of mouse embryos. Using this technique we have begun to characterize the cellular mechanisms of duct elongation. Furthermore we have also examined the occurrence of oriented cell division in the nephric duct and established that it occurs during the late stages of duct elongation.

Keywords: Morphology, Nephric Duct, Live Imaging, Early Kidney development

Résumé

Les anomalies congénitales du rein et des voies urinaires sont parmi les défauts de naissance les plus communs. Une cause potentielle de ces défauts est l'incapacité du canal de Wolff a étendre pour atteindre le cloaque. Une meilleure compréhension du processus sera utile, dans le traitement, le diagnostic et la prévention des maladies. Nous avons établi des conditions appropriées pour l'image en direct d'embryons de souris. En utilisant cette technique, nous avons commencé à caractériser les mécanismes cellulaires d'allongement du canal de Wolff. En outre, nous avons également examiné l'apparition de la division cellulaire orientée dans le canal de Wolff et établi qu'il se produit pendant les derniers étapes de l'allongement.

Chapter I: Introduction

The development of the animal body plan is a fascinating and remarkable process that begins with the meeting of an ovum and a spermatozoon. Contained in these cells are the tools, primarily in the form of proteins, and information, in the form of nucleic acids, needed to build an animal body. But how does a series of nucleotides encode the blueprint of complex organs such as a brain or a kidney? How does an individual cell know what its place in the blueprint is? How can hundreds of thousands of cells coordinate with each other to form an organ? What happens if these processes go wrong? These are the type of questions developmental biologists seek to answer.

Developmental Biology in Context

The question of how the animal body is generated is perhaps surprisingly old, dating back to ancient Greece. The first recorded study of developmental biology dates to the 4th century BCE and the Greek philosopher Aristotle. From his studies of developing animals he deduced the function of the placenta and umbilical cord and hypothesized that organs develop in a specific order from more primitive tissues.

In the 17th century the invention of the microscope allowed biologist to observe developmental processes in greater detail than ever before, leading to a renewed interest in the field. Since this time, microscopy has remained an essential tool in developmental biology and advances in microscopy often led to advances in this field. Detailed anatomical descriptions of development were made for the chick, frog, and many other models. Experiments using microsurgery and tissue transplantation between parts of the embryo or between species led to an understanding of concepts such as patterning and commitment. In the early

twentieth century Nadine Dobrovolskaïa-Zavadskaïa was the first to show the relation of genetics to development, with the discovery of a gene, Brachyury, which was responsible for birth defects in mice (Dobrovolskaia-Zavadskaia 1927). Advances across many disciplines including genetics, cell/molecular biology and microscopy have continued to contribute to the study of development, which is now a widely researched field of biology.

A major reason to study developmental biology is its relevance to disease. Major congenital malformations occur in approximately 2.4% of births (Dolk et al. 2010) and are one of the leading causes of infant mortality (Mathews & MacDorman 2013). Such anomalies greatly increase early termination of pregnancy and approximately 2% of infants born with major defects die in the first week of life (Dolk et al. 2010). Congenital defects also represent a leading cause of morbidity in the adult population (McKenna et al. 2005) and a significant financial burden on the healthcare system (Russo & Elixhauser, 2006).

Studying development leads to a better understanding of how congenital defects arise and what the underlying genetic and environmental causes are. This in turn leads to new tools to be used in treatment, diagnosis and prevention.

The Kidney: A Model for Disease and Development

The kidney and urinary tract are among the organs most commonly affected by birth defects. Such defects are present in approximately 1 in 300 to 1 in 625 live births (Dolk et al. 2010; Wiesel et al. 2005). The urogenital system (UGS) is subject to a diverse array of malformations and such defects are a significant cause of

morbidity in children and adults leading to conditions such as renal failure, chronic kidney infection and hypertension.

The kidney also represents a good model system to study a wide variety of developmental processes. These include mesenchymal epithelial transition, collective cell migration, epithelial-mesenchymal interactions, epithelial tubulogenesis, and transcriptional networks. Furthermore, elements of urinary system development are conserved throughout vertebrate evolution, so it can be studied in a variety of model organisms. As such the urogenital system is an excellent model system to study organogenesis.

Anatomy of the Urinary System

Diseases of the urinary system represent such a large health concern because of the essential role the kidneys and urinary tract have in maintaining homeostasis in the body. Among its many essential roles the kidney is responsible for regulation of blood pH and salinity, excretion of waste and toxins and absorption of water and metabolites. Additionally the kidneys function as an endocrine organ secreting renin and erythropoietin (Vize et al. 2003).

The primary functional unit of the kidney is the nephron; nephrons are the point of interface between the filtration apparatus and the vascular system. In a single human kidney there are approximately one to two million nephrons (Vize et al. 2003). Within the nephron, blood serum passes from the microvasculature of the glomerulus to the kidney via ultrafiltration, the filtrate passes through a series of tubules which perform the excretory and reabsorbtion functions of the kidney (Vize et al. 2003). The filtrate then leaves the nephron as urine passing through the

collecting ducts, renal pelvis and ureter into the bladder. At the interface of the ureter and bladder the ureteric valve, together with the peristaltic movements of the ureter, ensures the one-way flow of urine from the ureter to the bladder. The bladder stores urine until it is time to void at which point the bladder smooth muscle contracts and urine is expelled through the final outflow tract, the urethra (Vize et al. 2003). (See Figure 1)

Overview of Renal Development

The kidney and urogenital system arise as a result of a complex series of developmental steps. In mammals it proceeds through three distinct stages, the pronephros, mesonephros and metanephros. Though only the metanephros is present in adult mammals each stage is important in the proper development of the kidneys.

The first step in the development of the kidney and urogenital system is the definition of the intermediate mesoderm and the induction of pronephros in the intermediate mesoderm. The intermediate mesoderm is a layer of mesoderm derived from the primitive steak that is formed between the paraxial mesoderm and lateral plate mesoderm at approximately embryonic day (E)8.5. Specification of the urogenital progenitor cells in the intermediate mesoderm is triggered by signals received from the roof plate, ectoderm and paraxial mesoderm (James et al. 2006; Mauch et al. 2000; Obara-Ishihara et al. 1999). These signals induce a population of cells to become renal progenitor cells that will then undergo mesechymal-epithelial transition to form the pronephric duct. (Figure 2 A,B)

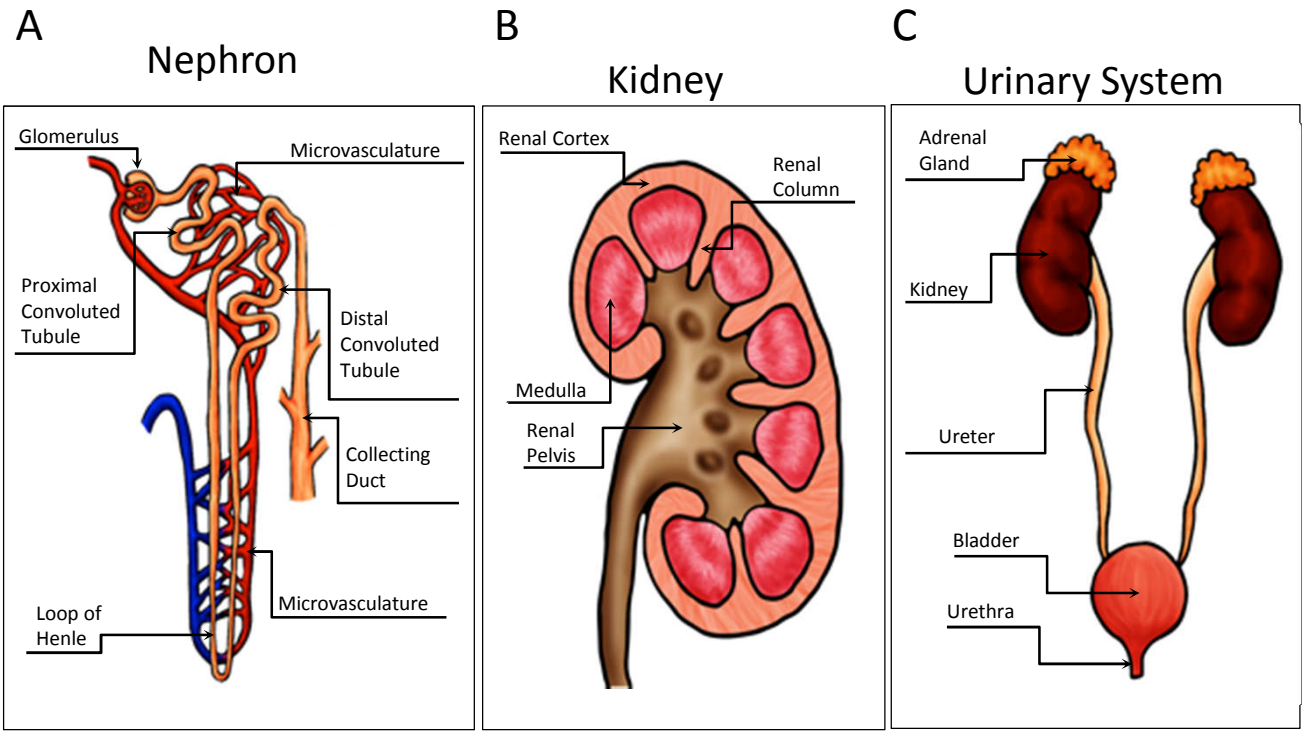

Figure 1. Illustrations of Kidney Anatomy.
A) The nephron is the basic functional unit of the kidney. Blood serum passes from the vasculature to the nephron at the glomus via ultrafiltration. This serum passes through a series of tubules that perform excretory and absorbtive functions of the kidney, and then enters the collecting duct as urine. B) A cross sectional view of an adult mouse kidney. The renal Cortex and renal column contain the glomeruli and convoluted tubules, while the cortex contains the loop of Henle and the collecting duct. The collecting ducts drain to the renal pelvis, which itself is drained by the ureter. C) Gross morphology of the urinary system. Urine is conveyed form the kidney to the bladder via the ureter. The bladder stores urine and is emptied by the urethra, which is the final outflow tract of the urinary system.

The pronephric duct matures into the pronephros, in some primitive fish this is the final form of the adult kidney. However, in most fish and in amphibians it forms a functional embryonic or larval kidney, and is later replaced by the mesonephros in adulthood. In amniotes, the pronephros is a transitional structure and never matures into a functional kidney. The development of the pronephros begins with the extension of the caudal end of the pronephric duct towards the cloaca. In fish and amphibians the pronephros continues to develop into a functional larval kidney. For example in *Xenopus Leavis* the rostral end of the pronephros matures to invade the coelomic cavity. Serum is filtered into the coelomic cavity by the glomus, an arteriole that splits off from the dorsal aorta and branches into a mass of capillaries. Opposite the glomus are the nephrostomes, which collect excreted waste. The waste is then carried out through the pronephric duct to the cloaca (Vize et al. 1997). (Figure 2 B,C)

The second stage of kidney development, the mesonephros, is the fully developed kidney of amphibians and most fish. While in amniotes, the mesonephros is transient and degrades before birth, in some species it does serve as a functional kidney during embryogenesis (Vize et al. 1997). The formation of the mesonephros begins with signalling between the nephric duct and the surrounding mesenchyme, the nephric cord. This signaling induces the condensation of the nephrogenic mesenchyme into mesonephric tubules. In the functional mesonephros these tubules will attach themselves to the nephric duct and mature into nephrons. Unlike the pronephros each tubule is vascularized by its own glomerulus. The glomerulus, like the glomus is a mass of capillaries responsible for excretion of serum into the

kidney. In amniotes, the mesonephros also contributes to the male genital system, namely the epididymis and vas deferens.

The final stage of kidney development is the metanephros. This is the functional kidney in mammals, birds and reptiles. The formation of the metanephros begins with signaling between the nephric duct and surrounding mesenchyme, called the metanephric mesenchyme. This induces a swelling of the nephric duct epithelium, which resolves into the ureteric bud. The ureteric bud then invades the metanephric mesenchyme and branches. Reciprocal signaling between the ureteric bud epithelium and metanephric mesenchyme causes further branching of the ureteric bud into the ureteric tree (Dressler 2006)(see figure 2). Further reciprocal signaling between the ureter tips and metanephric mesenchyme induces epithelialization of the metanephric mesenchyme surrounding the tips into comma shaped bodies, which mature into S shaped bodies and ultimately become the metanephric nephrons. The ureteric tree becomes the collecting ducts, renal pelvis and ureter (Costantini & Kopan 2010). The ureteric bud remains attached to the nephric duct and the portion of the duct between the ureter and bladder, the common nephric duct, is eliminated by apoptosis, resulting insertion of the ureter in the bladder (Figure 2 D) (Uetani & Bouchard 2009).

Congenital Anomalies of the Kidney and Urinary Tract

Congenital anomalies of the kidney and urinary tract (CAKUT) are among the most common birth defects and such anomalies range in severity from being asymptomatic structural abnormalities to being causes of severe morbidity and mortality (Bulum et al. 2013; Renkema et al. 2011).

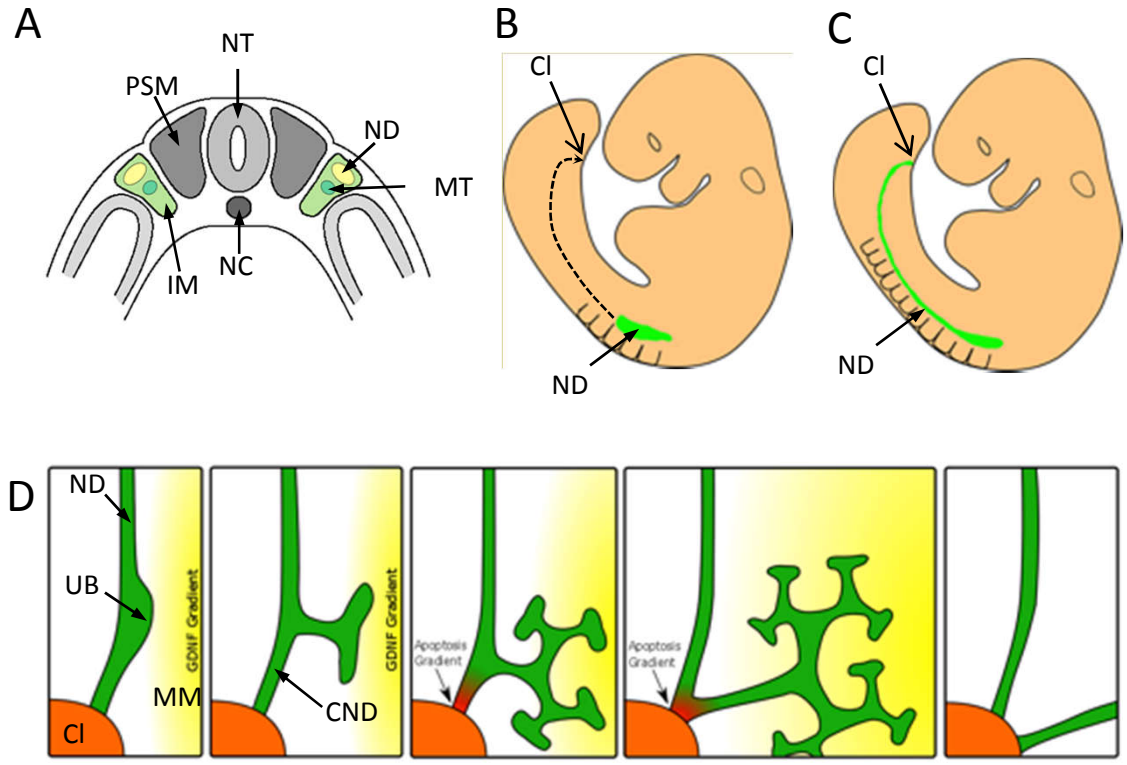

Figure 2. Early Development of the Mouse Kidney
A) At E8.5 the Nephric duct is induced in the intermediate mesoderm which lies between the pre-somitic mesoderm and the lateral plate mesoderm at the level of the forelimb bud. B,C) After induction the nephric duct extends from approximately the level of the forelimb bud the cloaca. D) Once the nephric duct reaches and fuses with the cloaca a GDNF gradient from the metanephric mesenchyme induces ureter budding and branching. During the elaboration of the ureteric tree, an apoptosis gradient starting from the cloaca results in a gradual elimination of the common nephric duct. This results in the insertion of the ureter in the cloaca. NT – Neural Tube, NC – Notochord, So – Somites, IM – Intermediate mesoderm, ND – Nephric duct, Cl – Cloaca, UB – Ureteric Bud, CND – Common Nephric Duct, MM – Metanephric Mesenchyme

This disease group includes a diverse array of anomalies including renal agenesis, vesicoureteral reflux (VUR) or the reverse flow of urine from the bladder into the kidney, hydronephrosis or the swelling of the kidney due accumulation of water in the kidney, ureteropelvic junction obstruction (UPJO) a blockage between the renal pelvis and ureter, vesicoureteral junction obstruction (VUJO) a blockage between the ureter and the bladder, duplex kidney, horseshoe kidney, cystic kidney, duplex ureter, and renal hypoplasia (Renkema et al. 2011; Song & Yosypiv 2011). These conditions result in a variety of symptoms including incontinence, painful urination, urinary tract infection, kidney stones and renal failure. In children CAKUT is the single largest contributing factor to chronic kidney disease (CKD) and end stage renal failure (Kerecuk et al. 2008; Renkema et al. 2011; Sanna-Cherchi et al. 2009). Furthermore, malformations that are asymptomatic in childhood may present as hypertension, proteinuria and renal disease in adulthood (Kerecuk et al. 2008). By understanding the morphogenic process of development we can see how defects result from errors in these processes.

In addition to understanding the morphogenic processes involved it is equally important to examine the underlying molecular and genetic processes. Some genes have been identified that associate with syndromes that encompass CAKUT. Such associations include *PAX2* with Renal coloboma syndrome (Sanyanusin et al. 1995), *GATA3* with hypoparathyroidism deafness and renal anomaly syndrome (Van Esch et al. 2000), *EYA1* and *SIX1* with Branchio-oto-renal syndrome (Kochhar et al. 2007) and *HNF-1β* with renal cysts and diabetes syndrome (Bingham & Hattersley 2004). Despite identifying these CAKUT associated genes, the genetics of CAKUT remains

quite complex. Some cases follow strict Mendelian inheritance patterns, others show familial clustering with variable penetrance and others are sporadic (Bulum et al. 2013). The complex genotype-phenotype relation underlying of CAKUT as well as the highly variable spectrum of phenotypes is due to the complex nature of kidney development and the intricate genetic network that controls it.

Molecular Basis of Kidney Development

One of the current challenges in understanding the development of the kidney is the dissection of the developmental processes on a molecular level. In this section, I will outline some key genetic components of early kidney development.

However, before discussing early kidney development we must consider the important development steps that set the stage. These are the specification of the intermediate mesoderm, the specification definition of the pronephric field in the intermediate mesoderm and the formation of the nephric duct from intermediate mesoderm cells. This induction of cells towards a nephric duct fate has been shown to be dependent on a variety of developmental signals (Figure 3a). Signaling from the anterior intermediate mesoderm is known to be required for the formation of the nephric duct (Barak et al. 2005). It also requires signals from the trunk paraxial mesoderm, these are necessary for expression of Pax2, which is the first marker of nephric duct fate (Mauch et al. 2000).The specification of the intermediate mesoderm is the first step we will consider. This requires signals from the surface ectoderm. However, exogenous BMP4 is capable of substituting these signals (Obara-Ishihara et al. 1999). BMP signaling was shown to correlate with intermediate mesoderm gene expression (James & Schultheiss 2005). Nodal like

signaling is also required for intermediate mesoderm gene expression and increases in Nodal signaling can cause an expansion of the intermediate mesoderm field (Fleming et al. 2013). These findings strongly implicate BMP signaling in the specification of the intermediate mesoderm.

Within the intermediate mesoderm transcription factors play an important role in defining the boundaries of the intermediate mesoderm. Like transcription factors *FoxC1/2* which play a role in defining the mediolateral axis of the intermediate mesoderm. Since, compound mutants for *FoxC1* and *FoxC2* show medially expanded expression of the early intermediate mesoderm marker *Lim1* (Wilm et al. 2004). Another transcription factor *HoxA6* seems to define the anterior boundary of the intermediate mesoderm by repressing intermediate mesoderm fate (Attia et al. 2012).

The definition of the pronephric field within the intermediate mesoderm is the next important step to examine. It has been shown that retinoic acid (RA) is required for this step. Inhibition of RA signaling disrupts pronephros formation and increased RA signaling expands the pronephric field (Cartry et al., 2006). RA also induces expression of HoxB4, which is known to expand the intermediate mesoderm field when expressed ectopically (Preger-Ben Noon, Barak, Guttmann-Raviv, & Reshef, 2009).

The outcome of this complex series of signals is the specification of the nephric lineage by the transcription factors Pax2 and Pax8 (Bouchard et al. 2002). Which are the key players in the next steps of kidney development.

Pax2/8

Pax2 is one of the most important transcription factors in kidney development. It is expressed during the development of the urogenital system, central nervous system, eye and ear (Dressler et al. 1990; Nornes et al. 1990; Püschel et al. 1992). *Pax2* is essential for kidney development as *Pax2* null mice display kidney agenesis as well as absence of genital tracts. In these *Pax2* null mice the nephric duct is specified and extends to the cloaca but the degenerates before ureteric budding, resulting in kidney agenesis (Torres et al. 1995). *Pax8* is another Pax gene expressed in the nephric duct that acts redundantly with *Pax2* (Bouchard et al. 2002; Heller & Brändli 1999). *Pax2/8* double heterozygote mice display severe kidney hypoplasia (Narlis et al. 2007) while mice with homozygous deletions for both *Pax2* and *Pax8* fail to even specify the nephric duct (Bouchard et al. 2002). This demonstrates that *Pax2* and *Pax8* are necessary for specifying the nephric duct (Bouchard et al. 2002). *Pax2* is also necessary in the metanephric mesenchyme where it plays an important role in regulation of *Six2* and GDNF (Gong et al. 2007; Torres et al. 1995).

Lim1

The transcription factor Lim1 is another early marker of the nephric duct (Barnes et al. 1994; Fujii et al. 1994) and like *Pax2* it is essential for nephric duct development (Kobayashi et al. 2005; Pedersen et al. 2005; Tsang et al. 2000). Mice null for *Lim1* usually die at E10, however the few that survive to birth lack kidneys and gonads among other phenotypes (Shawlot & Behringer 1995). If the lethality phenotype is bypassed by conditional deletion of *Lim1* in the nephric duct using $Pax2^{cre}$, elongation of the nephric duct is delayed and budding and branching are reduced.

This results in hypoplastic kidneys, hydronephrosis and in some cases kidney agenesis (Pedersen et al. 2005). In another conditional knock-out in the nephric duct, by *HoxB7*^{cre}, ureteric budding fails and the nephric duct degrades, (Kobayashi et al. 2005). *Lim1* is also necessary at later stages of kidney development in nephron formation (Kobayashi et al. 2005). Interestingly, it has been shown that *Pax2* is necessary for the expression of *Lim1* through direct transcriptional regulation (Boualia et al. 2013; Bouchard et al. 2002).

Gata3

Gata3 is the third key transcription factor that is required for normal nephric duct morphogenesis. Interestingly, *Gata3* like *Lim1* is a direct transcriptional target of Pax2/8 (Boualia et al. 2013; Grote et al. 2006). *Gata3* null mice display kidney agenesis due to a failure of the nephric duct to reach the cloaca. In such mice the nephric duct completely fails to extend and becomes hyperproliferative, or it begins elongation but is misguided, going towards the surface ectoderm rather than the cloaca (Grote et al. 2006). It has also been shown that Gata3 is also necessary for ureteric bud outgrowth. In conditional mutants for Gata3 in the nephric duct *Gata3* negative cells are unable to contribute to the ureteric bud (Grote et al. 2008). One of the critical targets of Gata3 that has been identified is the receptor tyrosine kinase *Ret*, which is critical for budding and branching of the ureteric bud (Grote et al. 2008).

Pax2, *Lim1* and *Gata3* together form the core transcriptional network underlying early nephric duct development. *Gata3* and *Lim1* have been shown to regulate each other, with direct regulation of *Lim1* by *Gata3*, this forms a bi-stable positive

feedback loop, resulting in stable expression of both Gata3 and Lim. Furthermore, as *Pax2/8* lies upstream of both *Lim1* and *Gata3* it acts as a switch to activate this feedback loop between *Gata3* and *Lim1* (Boualia et al. 2013). A host of other transcription factors such as *Id4*, *Emx2* and *Evi1* lie downstream of this core network element, as do effector genes such as *Ret*, *Npnt*, *Pcdh19* (Boualia et al. 2013) (See Figure 3b, 3c).

Metanephric Mesenchyme

While the nephric duct is extending towards the cloaca the specification of the metanephric mesenchyme is taking place. This specification occurs via a transcriptional cascade starting in the intermediate mesoderm surrounding the nephric duct starting with the Transcription factors *Osr1* and Hox11 paralogs, *Hoxa11*, *Hoxc11* and *Hoxd11* (Gong et al. 2007; James et al. 2006; Wellik et al. 2002). These Transcription factors are at the top of a hierarchical cascade which activate a series of Transcription factors including *Eya1*, *Six1* and *Pax2* (James et al. 2006; Sajithlal et al. 2005; Gong et al. 2007). This cascade further activates Transcription factors including *Sal1* and *Six2* as well as effectors such as *Grem1* and *Gdnf* (Gong et al. 2007; Nie et al. 2011; Xu et al. 2003). These downstream effectors and Transcription factors are required for, among other things, normal ureter budding and branching and to prepare the metanephric mesenchyme to respond to signaling from the ureteric bud. (See Figure 3 d)

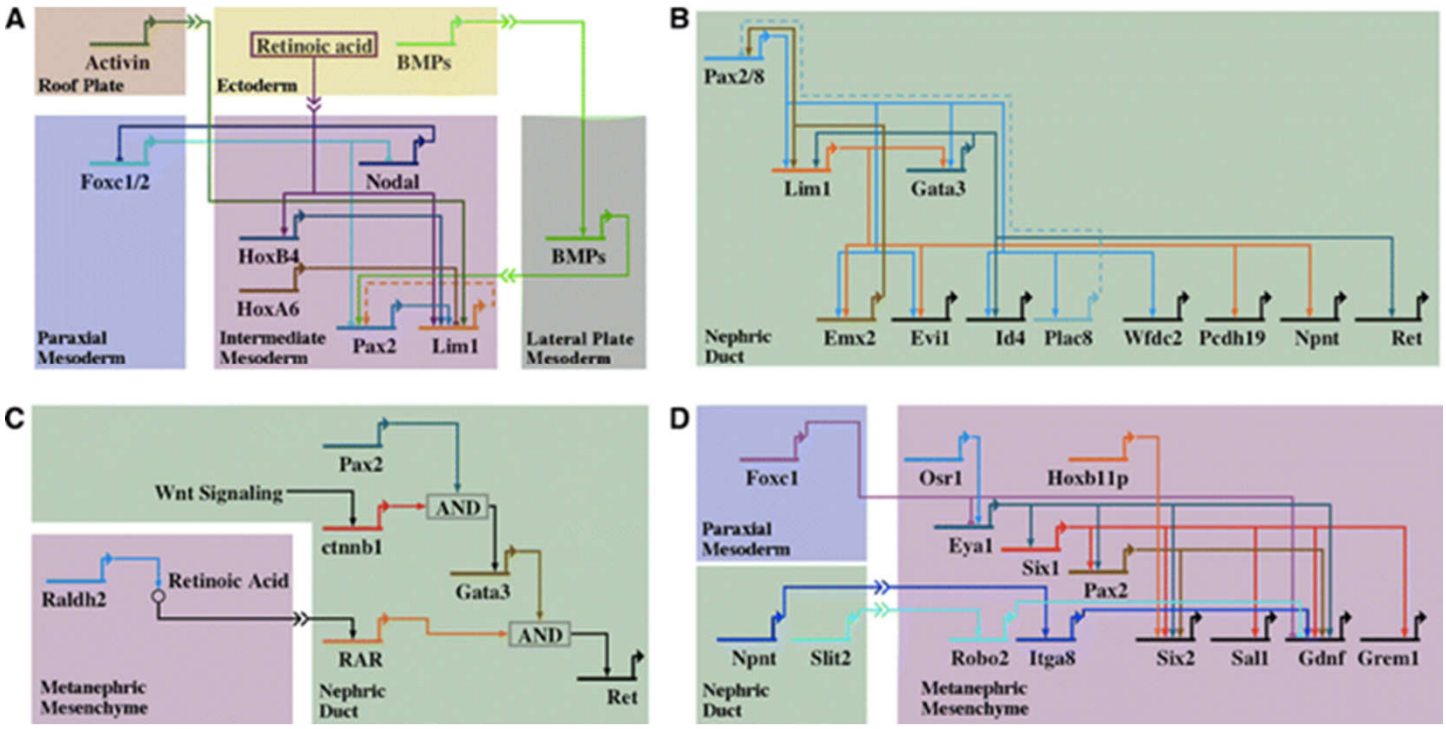

Figure 3. Key Gene Network Diagrams of Early Kidney Development
A) Transcriptional network in the pre-somitic mesoderm leading to the expression of Pax2 and Lim1 and the definition of the nephric duct. B) Pax2 activates both Lim1 and Gata3 whose expressions are then maintained by mutual activation. These three transcription factors control a host of downstream effectors. C) The Genetic Network controlling Ret expression on the nephric duct is analogous to a logic circuit; a series of logical AND gates determines RET expression. D) A transcriptional cascade controls GDNF expression in the Metanephric Mesenchyme.

GDNF-RET-WNT11: The Core Feedback Loop of Budding and Branching

One of the important outcomes of this cascade is the correct timing and positioning of *Gdnf* expression, which is critical to normal development of the kidney. Gdnf is secreted from the metanephric mesenchyme and acts on the receptor tyrosine kinase Ret and its co-receptor GFRα1 in the nephric duct This is the primary signal responsible for the evagination of the ureteric bud from the nephric duct and invasion of the ureteric bud into the metanephric mesenchyme. The ureteric bud in turn will secrete Wnt11, which feeds back to the metanephric mesenchyme to activate Gdnf signaling. This positive feedback loop between Ret, Wnt11 and Gdnf makes up the core of the reciprocal signaling between the ureteric bud and metanephric mesenchyme. (Figure 4)

The Gdnf-Ret-Wnt11 feedback loop is central in ureter budding, but significant amount of additional modulation is required to ensure normal budding and branching. One important regulator is Sprouty1, both a target of Ret signaling in the nephric duct and a Ret antagonist. As such it acts in an auto-regulatory negative feedback loop, providing an essential brake for the Gdnf-Ret-Wnt11 positive feedback loop (Basson et al. 2005). Limiting Gdnf expression is another important point of negative regulation. Activation of Robo2 in the metanephric mesenchyme by Slit2, the source of which is likely the nephric duct, acts to limit Gdnf expression to the posterior portion of the metanephric mesenchyme (Grieshammer et al. 2004). Negative regulators also interact with other positive regulators in order to provide "fine-tuning" to the budding and branching program.

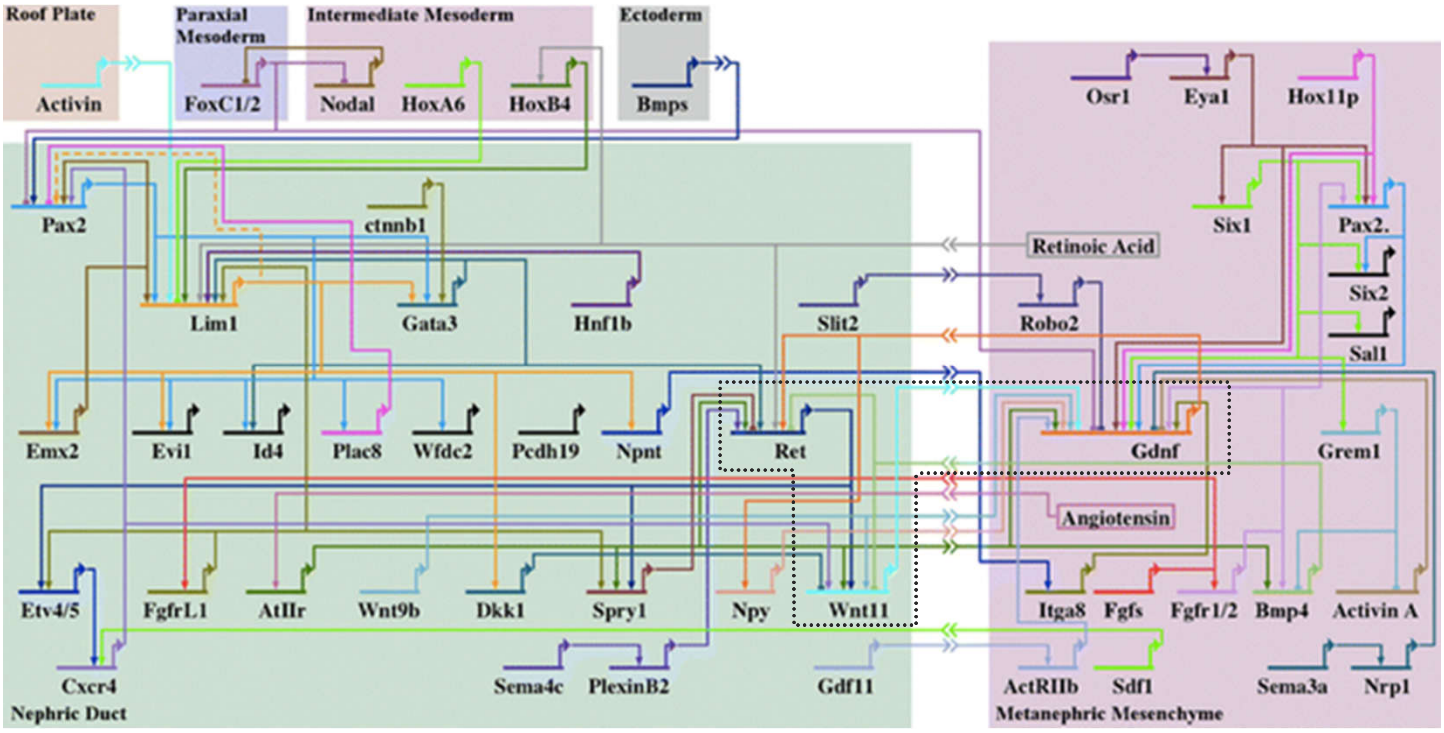

Figure 4. Comprehensive Network Diagram of Early Kidney Development. This figures illustrates core positive feedback loop of budding and branching between GDNF, RET and WNT11 (outlined by dotted line), the complex genetic network that is involved in establishing feedback loop, and the complex network involved in the modulation of this feedback loop.

For example, Bmp4 is expressed in the mesenchyme surrounding the nephric duct where it acts as a negative modulator of the GDNF-Ret-Wnt11. However Gremlin1, a Bmp antagonist, opposes Bmp4 activity allowing the ureteric bud to overcome Bmp4 driven inhibition and ensuring correct positioning of the bud (Michos et al. 2007).

Positive regulators are required for full elaboration of the ureteric tree, they also add a level of robustness and fine tuning. The Fgf family of growth factors seems to play an important secondary role in budding and branching. *Fgf7* mutant mice have smaller kidneys and it was shown Fgf7 modulates ureteric bud formation (Qiao et al. 1999). Interestingly, mice null for *Gdnf* and *Spry1* form a full sized but abnormally branched kidney. However, in mice null for *Fgf10* as well as *Gdnf* and *Spry1* this branching is completely abrogated. *Fgf10* was shown to be necessary for normal ureteric branching in *Gdnf* heterozygotes (Michos et al. 2010). *Fgf8*, *Fgf9* and *Fgf20* have been implicated in kidney development as well as the Fgf receptors *Fgfr1*, *Fgfr2* and *FgfrL1* (Attia et al. 2012; Atsuta & Takahashi 2015; Barak et al. 2012; Hains et al. 2008; Zhao et al. 2004; Hains et al. 2010; Gerber et al. 2009). Furthermore FGF family members, *Fgf1*, *Fgf2*, *Fgf12*, are also expressed in the developing kidney. The number of Fgfs involved or expressed suggests that Fgf signaling may play a more important role in budding and branching than is currently understood. However, redundancy between Fgf family members makes this role difficult to fully characterize.

Several other factors have been identified that modulate the core Gdnf-Ret-Wnt11 feedback loop, including *Gdf11*, *Npnt*, *Itga8*, *Npy*, *Sema4c*, *PlexinB2*, *Sema3*, and

Activin A (Choi et al. 2009; Esquela & Lee 2003; Linton et al. 2007; Maeshima et al. 2006; Perälä et al. 2011; Tufro et al.). The number and diverse nature of such regulators serves to highlight the complexity of the regulation of budding and branching.

Methods of Duct Elongation

Many disease states can result from errors in elongation of the nephric duct. If the nephric duct does fail to elongate or does not reach the right level of the metenaphric mesenchyme in a timely manner, the kidney will not form. If extension is delayed, the path of extension is misguided or nephric duct extension is otherwise disrupted, various congenital conditions can occur such as VUR or hydronephrosis. Although there is a significant disease risk associated with defective duct elongation there is a considerable gap in the knowledge of how exactly the duct elongates. As such, the focus of this project is to examine nephric duct elongation and gain a better understanding of the morphogenic and molecular mechanisms at work.

Once the first cells of the nephric duct are specified, growth of the duct occurs primarily by proliferation. Duct morphogenesis requires these newly made cells arrange themselves correctly within the structure of the duct. This can occur concurrently with cell division by oriented cell division or cell division by cell rearrangement.

Cells may contribute directly to growth during cell division. This requires the mitotic spindle to orient with the axis of tissue growth. Via oriented cell division (OCD) new cells will be generated by proliferation and contribute directly to tissue growth concurrently with cell growth. The mitotic spindle can orient itself with the

apical basal axis, however in the case of the nephric duct it must orient itself in the plane of the epithelium, potentially requiring the planar cell polarity (PCP) pathway. Interestingly PCP dependent OCD has been shown to occur in the postnatal development of the renal tubules (Nishio et al. 2010; Yu et al. 2009).

An alternative to oriented cell division is for cell rearrangement to occur after mitosis has been completed. The best characterized form of cell rearrangement is convergence and extension by intercalation. This consists of cell convergence in the axis perpendicular to cell growth causing the structure to become narrower in one direction but extend in the direction of growth. This is an important force in gastrulation and neurulation in several species. Convergence and extension can also occur via multicellular rosette formation and resolution, interestingly this mechanism occurs in kidney tubule elongation (Lienkamp et al. 2012).

It is also possible that both oriented cell division and convergence and extension are contributing factors for duct elongation. Both may contribute in part to correct morphogenesis or alternatively different stages of growth may require different mechanisms.

With either mechanism, cells must be able to orient themselves with respect to the direction of duct growth, which lies in the plan of the epithelium. This requires the planar cell polarity pathway, which defines and maintains directional information in the axes of an epithelial sheet or tube. Planar cell polarity proteins are classified in three groups the global PCP pathway the core PCP pathway and the effectors of PCP. The global PCP pathway maintains polarity between cells and at the tissue level. The core PCP pathway regulates polarization cell autonomously. The effectors of PCP

relay the signaling from the core and global pathways. Interestingly each of the PCP pathways has been implicated in various stages of kidney development. *Wnt9b*, and *Fat4* are involved in postnatal development of the renal tubules in mice (Karner et al. 2009; Saburi et al. 2008). *Pkd1* inducible knockout mice, a model for polycystic kidney disease, exhibit misregulation of PCP proteins Fz3 and CDC42 as well as randomization of oriented cell division (Luyten et al. 2010). *Vangl2* has been shown to be required for kidney branching morphogenesis (Yates et al. 2010). *Daam1* is required for PCP signaling in the development of pronephric tubules in *Xenopus leavis* and Zebrafish (Miller et al. 2011).

Another form of polarization, which is in some ways similar to that seen in PCP, is the polarization that occurs in migrating cells. In this case the directional information is external to the cells, provided by diffusible gradients or signals on the substrate of migration. Epithelial cells sometimes migrate together while maintaining cell-cell contact, this is called collective cell migration. Collective cell migration occurs in various developmental systems, angiogenesis, wound repair, and in some metastatic tumors. There also exists a variety of types of collective cell migration (Friedl & Gilmour 2009). The polarization of cells associated with migration has shared aspects with PCP, and as the nephric duct is migratory this may contribute to polarity in the duct.

Project Objective

The kidneys and urogenital tract are important organs that are particularly prone to developmental defects. There are many unanswered questions concerning the early stages of kidney development. Particularly the morphogenic mechanisms at play in

nephric duct elongation, as well as the underlying genetics, are largely unknown. This step is an essential process in the formation of a healthy urogenital system. Problems in this stage of development could potentially be the cause of various birth defects, including severe conditions such as kidney agenesis.

The goal of this thesis was to advance our understanding of the molecular and cellular mechanisms by which the nephric duct extends from the intermediate mesoderm at the level of the forelimb bud through a growing structure to reach the cloaca. We examined the elongating duct *in-vivo* using live imaging techniques. We additionally investigated potential roles of: oriented cell division, convergence and extension and planar cell polarity.

Chapter II: Materials and Methods

Mice

Pax2^{gfp} (Pfeffer et al. 2002) were maintained on a C3H/He background for live imaging experiments. To generate *Pax2*^{Gfp} *Gata3*$^{\Delta}$ and *Pax2*^{GFP} *HoxB7*^{cre} *Gata3*^{flox} mice were backcrossed into a C57/Bl6 background.

Gata3^{gfp} mice have been previously described (Grote et al. 2006) and were maintained on a C3H/He background.

Gata3^{flox} mice have been previously described (Grote et al. 2008) and were maintained on a C57/Bl6 background.

Gata3$^{\Delta}$ mice have been previously described (Grote et al. 2008) and were maintained on a C57/Bl6 background.

HoxB7^{cre} were purchased from Jackson lab, and have been described previously (Yu et al. 2002) and were maintained on a C57/Bl6 background

Pax8^{cre} have been describe previously (Bouchard et al. 2004) and were maintained on a C3H/He background.

Vangl2^{lp} mice were obtained from our collaborator Dr. Phillipe Gros, and were crossed to a C3H/He background.

Rosa26^{cnf} were purchased from purchased from Jackson lab (Snippert et al. 2010) and maintained on a C57/Bl6 background.

Z/EG mice were purchased from Jackson lab (Novak et al. 2000) and maintained on a C57/Bl6 background.

Phosphorylated Histone H3 Staining

Pax2^{GFP} positive embryos were dissected between E9.0 and E9.5. Embryos were fixed in 4% paraformaldehyde for 1hr at room temperature (RT). Then they were washed twice for 5 minutes in PBST (Phosphate buffered saline 0.1% Tween) and permeabilized in 0.3% PBST – Trition X-100 for 30 minutes. Embryos were washed with 100mM PBS glycine twice at 5 minutes at RT and once for 10 minutes at RT. Following this embryos were washed twice in PBST. Blocking was performed in PBST with 0.1% Triton x-100 and 10% normal goat serum for 1 hour at room temperature. Primary antibody was added in PBST 0.1% Triton 5% Normal Goat Serum and 1:500 rabbit anti-phosphorylated histone 3 (ser10) from Millipore (Cat# 06-570) and incubated overnight at 4°C. Embryos were then washed three times for 15 minutes in PBST. Alexa-568 conjugated goat anti-rabbit antibody from Invitrogen (Cat# A-11036) was added along with DAPI 1:500 and incubated at room temperature for 1 hour. Embryos were then washed three times for 15 minutes in PBST and mounted with aqueous mounting medium or slowfade gold. In order to image both nephric ducts embryos can be mounted between two coverslips using funtak as a spacer to prevent embryos from being flattened. The coverslip is then attached to the slide with tape. This way the coverslip can be turned around allowing both nephric ducts of an embryo to be imaged.

Measuring the Rate of Proliferation

For measuring the rate of proliferation Z-stacks were acquired at different focal planes to ensure the entire depth of the duct was imaged. The resolution in the z-plane was 2.3 microns, which should ensure that every cell in the duct is imaged at

least once. During imaging a small overlap was left between frames at each edge of the frames. This enables alignment of consecutive frames so that it is possible to tile frames together and recreate a mosaic image of the entire length of the duct. PH3 positive cells within the duct as well as DAPI positive cells within duct were counted using the ImageJ cell counter plugin. The coordinates of each cell counted were recorded. Frames were tiled together into a mosaic using the ImageJ MosaicJ plugin and a mosaic image of the entire length of the duct was generated. The approximate distance between the tip of the nephric duct and the closest edge of each frame to the tip was measured on the mosaic image. Then the distance between each duct cell and mitotic duct cell was calculated relative to the edge of the frame. In this way we obtained the approximate distance of each cell to the tip of the duct.

Measuring the Angle of Mitosis

Using the imaging software Imaris or ImageJ, we rendered each spindle of the mitotic cells. Using the ImageJ object counter 3D plugin we rendered each spindle or post-mitotic cell, and recorded the volume and position data for the center of mass of each object. In order to make rendering faster and reduce the memory load on the computer the regions containing the mitotic cells were cropped and the position of the cropped area was noted and added to the coordinates obtained by the object counter 3D plugin. If cells register as multiple objects we calculated the volume-weighted centroid of the disparate objects that constitute each cell and use this as the center of mass of the cell. The difference between the centers of mass of each spindle/post-mitotic cell in 3D is the vector of mitosis. A similar rendering was done for the portions of the duct that flank the mitotic cell. In Imaris we rendered each

flanking section as a region of interest with consistent dimensions. In ImageJ we cropped out the section of the duct around the mitotic event. Then an area of the image between the two extremes of the duct was cleared or deleted, ensuring each section at the edge of the cropped image has the same width. Then using the object counter 3D plugin we obtained the center of mass as above. The difference in position between the two portions of the duct results in the vector of the duct. The dot product of the vector of the duct and the vector of mitosis was used to solve for the angle between the vectors.

$$\frac{A_x \times B_x + A_y \times B_y + A_z \times B_z}{\sqrt{A_x^2 + A_y^2 + A_z^2} \times \sqrt{B_x^2 + B_y^2 + B_z^2}} = cos(\theta)$$

Where θ is the angle between the vectors, A_x, A_y and A_z are the x, y and z components of the mitotic vector and B_x, B_y and B_z are the x, y and z components of the ductal vector.

Note that angular data does not follow normal distributions and as such student's T-test is not applicable. To test the significance of our data we have used the Kolmogorov-Smirnov test and the Mann-Whitney U-test. Both of these tests are non-parametric and as such do not require the data to follow a specific distribution. Both of these test are established in the literature as ways to test the significance of data sets of angles in the context of oriented cell division (Karner et al. 2009; Luyten et al. 2010; Nishio et al. 2010; Saburi et al. 2008).

Data Analysis for Convergence and Extension

In order to estimate the presence of convergence and extension in the nephric duct from the confetti mouse the positions of the cells was tracked with respect to the

center of the duct. If the distance between a cell and the center of the duct decrease it would indicate convergence and extension was occurring. In order to estimate the center of the duct we performed a 3D least squares linear regression (Jacquelin 2011) using the position of each cell in the duct as input. This method will result in two points that will define the line of regression. The distance between each cell and the regression line was then used to track convergence of cells towards the center of the duct. From the triangle formed by the two points of the line of regression and the point of interest, the center of mass of a cell, the shortest distance from the point of interest to the regression line can be obtained from Heron's formula and from the standard formula for the area of a triangle with the base of the triangle being the side between the points defining the regression line.

In-Situ Hybridization Protocol

Several *in-situ* probes were obtained from the Bouchard laboratory database or obtained from collaborators. Generation of the Ret probe are described in (Pachnis et al. 1993) and generation of the Raldh2 probe are described by (Batourina et al. 2001).

Live Imaging Protocol

The methodology for live imaging of the developing pronephros was published in in Methods in Molecular Biology. It represents a significant publication during this Master's degree and will be described in detail in the following chapter.

Semi-Quantitative PCR

Primers were generated using primer three and verified to be specific using BLAST. Embryos were dissected at embryonic day 9.5 and all tissue posterior to the forelimb bud was removed for RNA extraction. This RNA was reversed transcribed to generate cDNA. Three tenfold dilutions of this cDNA was used in the semi-Q PCR. (See Supplementary table 1).

Chapter III: Live Imaging of the Developing Mouse Mesonephros

Introduction

A description of this technique was published "Live imaging of the developing mouse mesonephros" by David Grote, Michael Marcotte and Maxime Bouchard in Methods in Molecular Biology (Grote et al. 2012). My contributions to this publication include the refinement and optimization of the method, preparation of figures and the writing of the materials, methods and notes sections of the publication.

Microscopy has had a major impact on the advancement of the field of developmental biology and it remains an indispensable tool in its study. Most imaging technologies are adapted for use with fixed tissues. However, embryogenesis is highly dynamic, and as such still images of fixed tissue only provide limited information about such process. In order to better study the developing nephric duct we have established imaging techniques to follow development of the nephric duct within live embryos. Live imaging will allow measurement of the dynamics of nephric duct morphogenesis, which are inevitably lost when imaging of fixed tissue. This chapter will describe the published method and expand on it by providing additional techniques, useful information and context for the importance of this technique.

Materials

Embryo culture Media:

1. Fetal bovine serum.

2. ddH2O.

3. 1 M Hepes, pH 7.2.

4. DMEM/F12 1:1 nutrient mix (without Hepes, without phenol red, with l-glutamine).

5. 200 mM l-Glutamine.

6. Penicillin–streptomycin (pen–strep) (penicillin 10,000 units/mL and streptomycin 10,000 μg/mL).

7. Rat serum: Rat serum can be purchased commercially; however, we recommend preparing your own rat serum as we have met with limited success using commercially available products. Rat serum should be prepared according to institutional and national animal care regulations. In our institution, rat serum is prepared as follows.

(a) Male rats are used as female hormones can interfere with embryo development. Rats are anesthetized with isoflurane in a controlled flow anesthesia chamber until unresponsive and not flinching when pinched on the foot with forceps. When unresponsive, lay the rat on its back and continue to dispense anesthesia using a nose cone.

(b) Make an inverted V-shaped incision in the abdomen to open the abdominal cavity. Move the intestines to reveal the dorsal aorta and vena cava. Carefully remove fat and connective tissue from the dorsal aorta and vena cava to create an opening over the vessels. It can be difficult to distinguish between the vena cava and dorsal aorta which both run parallel down the back of the abdominal cavity. The dorsal aorta is the more pink than the vena cava.

(c) Using a 20-mL syringe and a beveled 21-gauge needle, insert the needle bevel down into the dorsal aorta. Keep the needle in line with the aorta. Draw plunger

back slowly to match the rate of blood flow. Drawing the plunger too quickly may result in hemolysis. This has a strong negative affect on serum quality. Each rat should yield about 15 mL of blood.

(d) Collect blood in 15-mL conical tubes and put on ice.

(e) Ensure that rat is dead by severing the heart completely.

(f) Spin the blood in conical tubes at 1,500 × g for 5 min to pellet red blood cells.

(g) Using curved forceps, pinch and squeeze fibrin clot to release serum.

(h) Spin again and remove fibrin clot.

(i) Pool serum into 50-mL conical tubes and spin again to remove any remaining red blood cells.

(j) Aliquot into 5-mL aliquots in 15-mL tubes and freeze at −80°C.

Equipment

1. On-stage incubation chamber (e.g., Chamlide TC with TC adaptor for chambered coverglass from Live Cell Instruments) Two main types of incubation system are available: incubators that fit on the stage and those that enclose the optics system. Those that enclose the optics system provide greater environmental stability but are more expensive and take longer to equilibrate. (Figure 5a).

2. Gas flow and temperature regulator for on-stage incubation chamber (e.g., CU-105 gas flow and temperature controller from Live Cell Instruments).

3. 8-well-chambered cover glasses (e.g., Lab Tek II chambered coverglass system from NUNC) (Figure 5b).

4. CoverWell perfusion chamber gaskets, eight chambers, 9 mm diameter, 1 mm deep (Invitrogen) (Figure 5c).

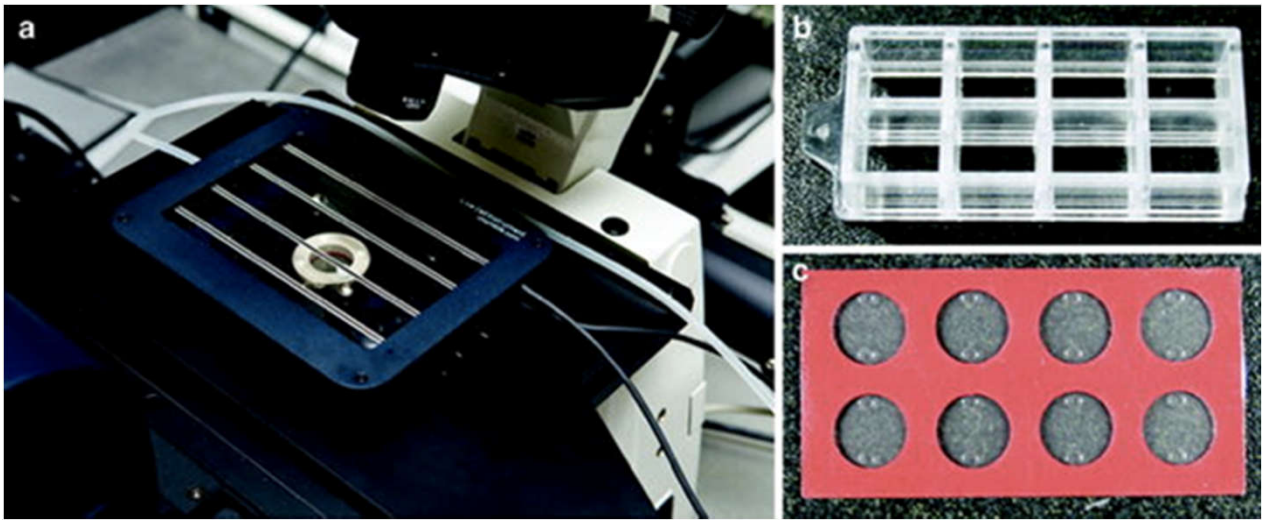

Figure 5. Basic Imaging Supplies.
(a) On-stage incubator setup. (b) Lab-tek II 8 well chambered coverglass. (c) 8-well cell perfusion gaskets.

5. CoverWell perfusion chamber gaskets, eight chambers, 9 mm diameter, 0.5 mm deep (Invitrogen).

6. Confocal microscope: Leica DMI 6000 B with a 20× plan-apochromat 0.75 numerical aperture air objective. The choice of objective will affect resolution and the depth into the tissue that can be imaged. Objectives with higher numerical apertures will have better resolution but generally will have a shorter working distance and will not be able to image as deep into the tissue. Quorum WaveFX Spinning Disc confocal system, Hammamatsu image EM camera Many microscope systems are available. Point scanners comparable to the Zeiss LSM 710 are good when imaging multiple colors; however, they are limited in their maximum speed. Line scanning microscopes, such as the Nikon live scan swept field confocal, and spinning disk microscopes, such as the system described above, can be used for high-speed imaging. This is ideal for imaging events that occur on short timescales. It is also useful if imaging a large number of Z-stacks and a large number of embryos, as it will lower the minimum interval between time points. Two photon excitation systems and selective plane illumination systems are optimal for imaging structures deep within the embryo. We elected to use a spinning disk confocal because its fast acquisition time allowed us to minimize laser exposer while imaging large z-stacks on multiple embryos within the necessary timeframe to observe developmental events.

8. 491 nm 25 mW diode Laser. The frequency of the laser light being used can influence embryo viability. Higher frequency light is more phototoxic. However, infrared light may harm the sample by heating it. .

7. Gas mixture: 40% O2, 5% CO2, 55% N2.

8. Dissecting microscope (e.g., Stemi-2000 stereo microscope from Zeiss).

9. Heating plate for dissections (e.g., Heatable universal mounting frame KH-L from PeCon).

10. Temperature regulator for heating plate for dissections (e.g., Tempcontrol 37 analog 1 channel temperature regulator from PeCon).

11. Cell culture incubator (37°C, 5% CO2).

12. Digital Monitoring thermometer with a cable and small probe suitable to measure temperature within chambered cover glass wells.

13. Pyrex petri dish, 60 × 15 mm. Glass dissecting dishes are used as glass cannot be scratched and will not damage dissecting tools.

14. Cell culture dish, 35 × 10 mm.

15. Hair tool: To make the hair tool, sterilize a piece of hair about 4-cm long in 70% ethanol, break the end of a glass Pasteur pipette to shorten it, and use melted paraffin to attach the hair to the end of the pipette.

16. 37°C water bath.

17. Two pairs of Dumont #5 forceps.

18. Fine iris scissors—Straight.

19. Sharp Surgical Scissors—Straight.

20. Plastic transfer pipettes.

21. Mineral oil certified for embryo culture.

Methods

Preparative Steps

The dissecting media and culture media must be prepared at least 4 hours in advance of imaging to allow the media sufficient time to warm to 37°C. To prepare the dissecting media add 4 mL of heat-inactivated (heated for 30 min at 56°C) fetal bovine serum to 45 mL of DMEM/F12 1:1 nutrient mix (without Hepes, without phenol red, with l-glutamine) in a sterile 50-mL conical tube. Then add 500 µL of 1 M Hepes buffer, pH 7.2 and 500 µL of penicillin–streptomycin (Penicillin 10,000 units/mL and streptomycin 10,000 µg/mL). Mix thoroughly by inversion and filter through a 0.2-µm filter. To prepare the culture media add 4.9 mL of heat-inactivated (30 min, 56°C) rat serum to 4.9 mL of DMEM/F12 in a 15ml conical tube. Then add 100 µL of 1 M Hepes pH 7.2 and 100 µL of penicillin–streptomycin. Again mix by inversion and filter through a 0.2-µm filter. Note that if the DMEM/F12 mix used in these media is more than 6 weeks old the L-glutamine may have expired. In this case it is necessary to add additional L-glutamine. If so add 500µL of 200 mM l-glutamine to the dissecting media and 100 µL of 200 mM l-glutamine to the culture media before filtration. Either media can be prepared up to sixteen hours in advance and stored at 4°C.

Certain steps must also be taken in order to prepare the microscope. First, turn on the microscope and use the imaging software to calibrate the stage. Place the live imaging chamber on the microscope with the adaptor for chambered slides. Fill the humidifier with sterile ddH2O and put 500 µL of sterile distilled water in each well of an 8-well-chambered cover glass and place it in the incubation chamber on the

microscope stage. This allows the microscope stage to equilibrate while a second chambered cover glass is being prepared for imaging. Turn on the heating unit for the on-stage incubation chamber humidifier, and objective warmer. Because of environmental factors and any changes made to the experimental set up it is necessary to determine the correct temperatures to input to the heating devices.

Well in advance of the experiment set instruments to 38°C and allow the temperature on the stage to equilibrate. An on stage incubation system is less efficient than an incubator that encloses the entire microscope, as a result there is some heat lost between the incubation system and the culture media. As such the system may need to be set the instruments above the desired temperature to obtain the correct conditions in the media. In the case of mouse embryos the temperature settings of the heating unit should be set such that the system equilibrates at 37°C.

It is important to attain a consistent temperature while imaging. The ambient temperature can influence the temperature on stage as such it may be necessary to adjust the settings of the heating unit accordingly. To ensure that the desired temperature is attained on the stage insert the digital thermometer in one of the water-filled wells of the chambered cover glass and check that the temperature on the stage is 37°C. The temperature on the stage will likely be lower than the temperature settings on the instruments. If using an oil immersion objective, be sure to use oil designed for use at 37°C and to pre-warm the oil.

The device used to hold the embryos in place must also be prepared in advance to do this cut out one quarter of a cell perfusion gasket well (Figure 6a, b).

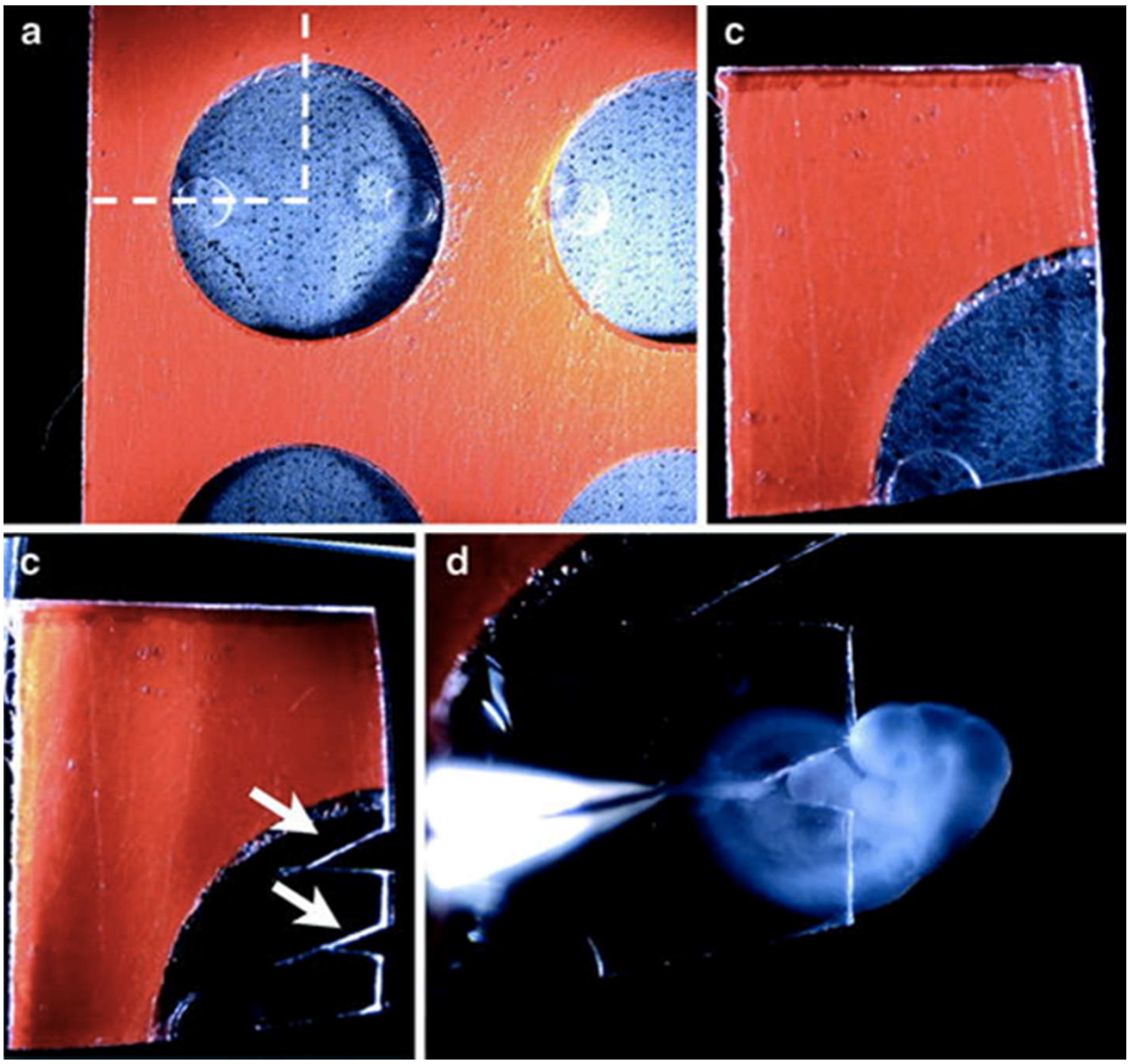

Figure 6. Preparation of Embryo Holder.
(a) Cell perfusion gaskets, cut a quarter of a well (dashed line) to make holder for embryo. (b) A quarter of one cell perfusion gasket well. (c) Use iris scissors to make small V-shaped cuts (white arrows) in the plastic surface of the cell perfusion gasket. (d) Place the embryo under the plastic surface of the gasket using the hair tool. Then, grasp the amniotic membrane with forceps and carefully wedge it into the V-shaped cut.

Use 0.5-mm-deep wells for E8.75–E9.0 embryos and 1-mm-deep wells for E9.0–E9.5 embryos. Make a V-shaped cut in the plastic surface of this quarter well about 1 mm by 3 mm (Figure 6c). Depending on the stage of the embryo, the size of v-shaped cut needed in the embryo holder may vary; if possible, cut two triangles of different sizes per embryo holder. Remove the strip of plastic from the gasket to expose the adhesive and place it on the bottom of the chambered cover glass.

Check the temperature and water levels in the cell culture incubator and water bath which should both be at 37°C. Pre-warm the dissecting media and culture media for at least 4 hours before the experiment. Put 500μL of culture media in each well of the prepared 8-well-chambered cover glass, put the rest in a 35-mm cell culture dish. Place the chambered cover glass and culture dish in the cell culture incubator.

Fill a 60-mm Pyrex petri dish with dissecting media and place it on the heatable universal mounting frame. Adjust the media temperature to 37°C using the digital thermometer to monitor the temperature. Pre-warm the remaining dissecting media, extra dissecting dishes and mineral oil in the cell culture incubator for at least 1 hour in advance.

The embryos must be incubated in a high oxygen high carbon dioxide environment use a gas mixture of 40% O_2, 5% CO_2, 55% N_2. This mixture should be attached to the incubation system and opened at least one hour in advance. Set the flow rate at a maximum of 10 lb. per square inch (psi). Keep the flow rate low to minimize evaporation of culture medium, which will strongly impact embryo viability. An appropriate flow rate may also need to be determined if the experimental set up is significantly altered.

The final preparative step is to turn on the laser. Most lasers take some time to achieve a stable output strength. As such the laser should be turned on about half an hour to an hour before starting imaging.

Dissection

Set up matings of the desired mice and check females for plugs to determine the first day of pregnancy. Sacrifice the pregnant mouse by cervical dislocation without anesthetic at the desired embryonic stage. Cervical dislocation is preferred as other methods of euthanasia may affect embryo development. Ensure that all preparations are complete before sacrificing the mother. Euthanize mice in accordance with institutional and national animal care regulations. Ask to be trained to do cervical dislocation from your animal facility.

Sterilize the abdomen with 70% ethanol then make an incision in the abdomen to expose the thoracic cavity. Move aside intestines to expose uterine horns. Occasionally, female mice that have plugged will not be pregnant. If possible, one should start multiple plug checks such that a second experimental mouse will be available on the day of the experiment should the first not be pregnant. If mice regularly plug but are not pregnant, the male may be infertile or conditions in the animal facility may be stressful to the mice, preventing them from becoming pregnant.

Cut out the uterine horns at the ends and at the level of the cervix, remove them and place them in pre-warmed dissecting media. Put the dissecting dish on the heating plate, from this point keep the embryos at 37°C. Place scissors on the uterine horn between each embryo, use tweezers to push uterus up between scissor blades, and

cut the uterus. Place each embryo in the pre-warmed 35-mm cell culture dish and add pre-warmed dissecting media.

Take one embryo at a time and dissect it in pre-warmed dissecting media in a 60-mm glass-dissecting dish. Perform the dissection very carefully as any damage to the embryo will severely compromise embryo viability. If unfamiliar with dissecting out embryos at this stage, it may be helpful to practice on less valuable samples.

Keep the dissecting dish on the heating plate and use the digital thermometer to monitor the temperature of the media. Maintain the temperature as close to 37°C as possible. Also note that blood and placental tissue will accumulate in the dissecting media. This may make dissections difficult. Change dissecting media for clean pre-warmed dissecting media when necessary and if necessary change to a clean dissecting dish. Use a small dissecting dish to conserve media.

To remove the embryos from the uterus insert fine forceps in the hole in the uterus which was made when the embryos were separated. Insert a second set of forceps and make a small tear in the uterus. Be careful not to apply pressure on the uterus: this may cause embryos to pop out of the uterus, which will damage the embryo. Very carefully continue to tear open the uterus until the placenta is exposed. Remove the placenta from the uterus and carefully pull it open with the fine forceps. Then remove the yolk sac from the placenta with the embryo inside. Again using forceps tear open the yolk sac and very carefully tear it off the embryo. If needed the yolk sac can be stored in PBS and used for genotyping. Once the yolk sac is removed from the embryo it will be directly exposed to the dissection media, which is not

optimal for embryo viability. Direct exposure to the dissection media can be minimized by working quickly.

Open the amniotic membrane and pull it away from the embryo, but leave it attached to embryo at the primitive gut. This is a good time to count the number of somites of the embryo to determine the exact developmental stage (for stages E8.0–E9.5).

Check for fluorescence, either using a fluorescent dissecting scope or the confocal microscope to be used. Place the embryos that express fluorescence in culture media. If the genotype of the embryos is needed, use the pre-warmed chambered cover glass with culture media to isolate the embryos. Otherwise, pool embryos in the 35-mm cell culture dish with pre-warmed culture media. Place the embryos in the cell culture incubator.

Embryo Placement

Cut the tip and of a plastic pipette so it is large enough to hold an E9.5 embryo and pre-flush the pipette with a small amount of culture medium. Use the pipette to transfer the embryos to the 8-well-chambered cover glass that contains the pre-warmed culture media. Place the chamber on the dissecting microscope in the heating plate that was used for dissections.

Use the hair tool to place the embryo under the clear plastic surface of the embryo holder next to the V-shaped cut, with the amniotic membrane facing the cut. Use fine forceps to grasp the amniotic membrane and the hair tool to manipulate the embryo. Carefully wedge the amniotic membrane into the cut in the plastic surface of the embryo holder gasket (Figure 6d). Proper positioning of embryo is critical for

obtaining good image quality. The closer the structure of interest is to the cover glass, the better the resolution will be. Additionally, proper positioning will ensure that the embryo does not become dislodged during imaging. After each embryo is correctly positioned add 60μL of mineral oil on the surface of each well and carefully mount the chambered cover glass in the on-stage incubator.

Imaging

Once embryos are mounted on the stage, open the image acquisition software. This experiment generates a large amount of data. Before starting image acquisition, verify that there is sufficient storage capacity available. This depends on the number of embryos imaged, the size of the z-stack, the resolution of the images, and the length of the experiment. The first time the experiment is performed ensure that there is ample storage capacity on the destination drive, at least 30GB is recommended. This first experiment can be used to estimate the amount of data generated per embryo per hour. Also note that certain imaging software programs will attempt to store data in the active computer memory which will likely cause the software to crash.

Set the Z-spacing according to Nyquist sampling rate. The required Nyquist sampling rate can be calculated online at http://www.svi.nl/NyquistCalculator. If the image is to be deconvolved a Z-spacing of one third the recommended Nyquist sampling rate must be used. Also for optimal deconvolution the Z-spacing should also extend several frames above and below the sample. Next set the interval between time points. The desired interval should depend on the nature of the processes being studied. The minimum interval time possible depends on the

number of samples being imaged and the capacity of the system being used. We use between 6 and 20 time points per hour for mesonephros development.

Locate the embryo and the structure of interest in bright field. Then switch to the appropriate laser, 491-nm in our case. Adjust the laser intensity, exposure time, and camera sensitivity to improve image quality, be sure to use auto-contrast to make this process easier. In order to avoid harming the embryos, laser intensity and exposure time should be minimized. Using lower laser power and exposure time may decrease resolution but could be necessary to keep embryos alive. Camera sensitivity and camera gain can be adjusted to improve resolution. Binning may also be used to decrease laser intensity and exposure time but at the expense of resolution.

If using an automated stage and multipoint imaging locate the structures of interest in each embryo. Focus on the structure of interest and save the coordinates in the imaging software. Before starting imaging check the focus and coordinates of each embryo to ensure they have not moved, note the imaging settings used (Laser intensity, camera gain, camera sensitivity, etc.) and start acquisition.

Once image acquisition is started, check on the experiment every 30–60 min to verify that the structure of interest remains in frame and that the embryos are surviving. If using an automated stage to image multiple embryos, there may be stage drift if the stage is not properly calibrated. This will cause embryos to move out of frame. For this reason, the stage should be properly calibrated. If the problem occurs, the experiment can be stopped and the position of each embryo can be reprogrammed in. Due to the motion of the automated stage and the motion of the

embryo caused by the beating of the heart, embryos may become dislodged from the cell perfusion gasket. If this occurs, image acquisition can be stopped, the chambered cover glass removed from the microscope, and the embryo repositioned. To monitor survival, check for a regular heartbeat and verify that there are no signs of necrosis. Under these conditions, embryos can survive up to 18 hours.

After image acquisition is complete, count the somites of each embryo and compare it with the count before the experiment to assess embryo growth. Back up data as soon as possible after the experiment.

Image Processing

Basic image processing can be done with specialized imaging software, such as Volocity (Improvision). Delete non-informative time points, such as out-of-frame images or unhealthy embryos. If embryos moved out of frame and the position needed to be reprogrammed in, images can be spliced together. 2D movies can be generated from a depth projection of z-stacks (Figure. 7, Supplementary Video 1).

Our deconvolution is done in Autoquant (MediaCybernetics) using blind iterative deconvolution. Try different deconvolution settings to identify what works best. Given that the distance of the embryo from the cover glass and the depth of the structure of interest within the embryo will vary for different embryos, the best settings may vary from sample to sample. For our samples the optimal settings were to use a theoretical point spread function and 15 iterations with a low noise level.

Deconvolved data can then be rendered with Imaris (Bitplane) to produce a 3D image or movie.

Discussion of Live Imaging

Mastery of this technique was a significant challenge and as such represents a major part of this Master's thesis. Credit is due to David Grote for the initial development of this technique. Aside from general optimization and development of this techniques specific contributions attributable to the author of this thesis include the development of methods to keep embryos stationary, the optimization of deconvolution and 3D rendering techniques, the development of the technique for use with the Z/EG (Novak et al. 2000) and Confetti mice (Livet et al. 2007), and the optimization of the swept-field confocal for use in live imaging.

The remainder of this chapter will discuss various things that must be considered in this technique that were not included in the paper. A consideration with regards to viability not discussed in the published paper is the stage of the embryo. The stage at which embryos are cultured should be determined by the experimental question being addressed. However, it is useful to keep in mind that earlier stage embryos are significantly easier to maintain in culture. Embryos that are E9.0 or younger are notably are less sensitive to changes in environmental conditions. Another consideration with respect to staging is how embryos should be positioned. Older embryos are often easier to position close to the coverslip with the technique described previously. When placing the gaskets, it is possible to bend the clear plastic surface of the gaskets towards the coverslip, which would allow smaller embryos to be positioned closer.

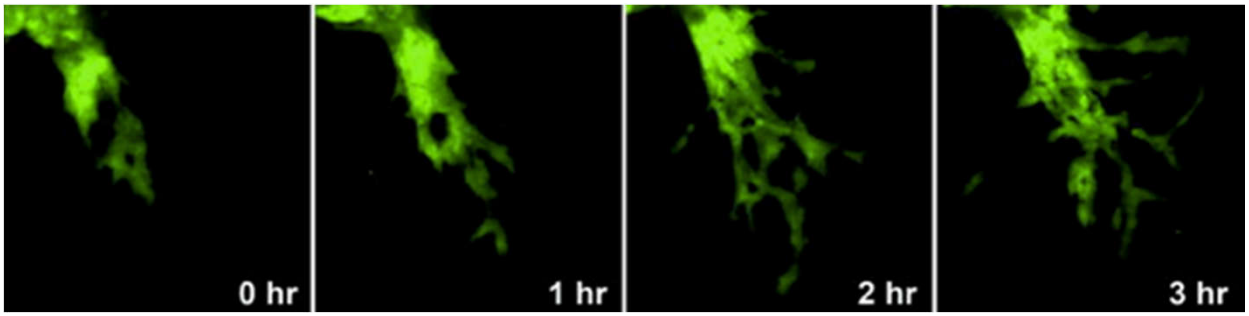

Figure 7. Time-lapse Imaging of Developing Pro/Mesonephros.
Pictures were extracted from time-lapse imaging of the growing mesonephros in E9.5 embryos. Fluorescence is obtained by GFP expression in mesonephric tissue using the Pax2GFP transgenic line.

As described in the paper much of the live imaging was done with the *Pax2*^{GFP} transgenic mice, which express GFP from the *Pax2* genomic locus in a BAC transgene (Pfeffer et al. 2002). This mouse likely contained multiple insertions of the transgene and as a result GFP is very highly expressed in the nephric duct of these mice. This allowed for high resolution imaging at low laser intensity. In addition to these mice, we used other genetically modified mice expressing fluorophores in the nephric duct. *Gata3*^{GFP} mice are a knock-in line expressing GFP from exon4 of the *Gata3* gene (Grote et al. 2006). However, in this line GFP was not expressed at sufficient levels to allow clear imaging of the nephric duct. The Z/EG mice express GFP from the *Rosa26* locus upon Cre mediated excision of a LacZ cassette. We crossed these mice to *HoxB7*^{cre} mice (Yu et al. 2002) which express Cre in the nephric duct at late stages of elongation. However, Cre activation is incomplete at this stage creating a mosaic expression pattern for GFP. This would in theory allow us to follow individual cells. However, levels of GFP expressed by the Z/EG allele were very weak in our system. This meant a drastic loss of resolution when compared the *Pax2*^{GFP} transgenic mice. In order to obtain the desired mosaic effect we tried using the Rosa26 confetti mouse strain (Livet et al. 2007), these mice stochastically expresses one of four fluorescent proteins when acted upon be Cre recombinase. These were crossed with *HoxB7*^{cre} and *Pax8*^{cre}, which deletes earlier in nephric duct development and more completely. With our imaging system we were able to image GFP, RFP and CFP but not YFP. However, imaging in three colors effectively triples exposure of the embryo to potentially harmful laser light, and as CFP requires use of a higher energy laser, it was not used experimentally. The

confetti allele generated the desired effect allowing the individual cells to be seen and tracked. While this system provided better resolution than *HoxB7*$^{Z/EG}$ it was still significantly poorer than the resolution obtained in *Pax2*^{GFP} mice. Having a highly expressed bright fluorophore is perhaps the single biggest determinant of image quality. The color of the fluorophore used must be taken into consideration. Longer wavelength or redder light is less energetic and as such is less phototoxic. However, as wavelengths lengthen into the infrared they begin to transmit heat to the sample, which can also be harmful. As such infrared light is less suitable for live imaging.

Another note with respect to staging not mentioned in the paper is resolution of structures at depth. In the case of the nephric duct this is not strictly necessary for earlier stages of development, however later in the development the rostral part of the duct is more difficult to image due to the tissue between the surface and the duct. It is worth noting that longer wavelength light also penetrates deeper. Making longer wavelengths more suited for imaging at depth.

Image Processing

Confocal imaging can be used to generate three-dimensional (3D) videos. This can be useful for a variety of reasons. For example imaging in 3D is necessary in order to accurately determine the angle of cell division. A two dimensional image of a cell dividing in a three dimensional structure will remove the z-axis component of the cell division vector (see methods). The result is that the measured angle will be less than the actual angle of division. In our experiments this would bias the angles to be in the same plane as the axis of nephric duct elongation. In the case of live imaging of the nephric duct 3D imaging revealed that the fillipodia we saw in static cultures

were always in the same plane, something that was not as apparent in other images. Renderings of the duct were done using Imaris. Once a rendering is created lots of useful data can be extracted from it. Positional data extracted from the renderings of the *Pax8*^{cre} *Rosa26*^{Confetti} mice were used to track cell movements. Depending on how the rendering is generated the positional data can be used to extract lots of other data such as, length and aspect ratio of extensions. These data can be further used to obtain things such as speed of elongation and retraction.

Such information could help determine the cellular mechanics of duct elongation. This information is also useful for comparing mutants and wild type mice. Notably the *Gata3* conditional knockout mice display a failure to correctly elongate. In the future this technique could be used to identify and quantify the differences in elongation rate, length of extensions and overall speed of growth between the *Gata3* null mice and wild type mice. This would greatly help in determining how *Gata3* is influencing elongation.

Detailed imaging of processes such as the elongation of the nephric duct can also lead to a broader understanding of epithelial morphogenesis in general. Furthermore, the conditions established here can be adapted to other organs in mice. Several interesting events are occurring at a similar developmental stage such as the development of the heart, somitogenesis and limb budding. Such live imaging is frequently done in other model organisms but this imaging setup allows for the dynamic processes of development to be studied in detail in an in vivo context in mammals.

Chapter IV: Mechanisms of Nephric Duct Elongation

Included in this chapter are figures and findings originally published in *Development* (Chia et al. 2011). My contributions to this paper included performing whole mount *In-situ* hybridization images for *Gata3, Ret, and Raldh2* probes in wild type and *Gata3* mutants, obtaining images of the cell extensions in wild type and *Gata3* mutants.

The important role of *Gata3* in the formation and elongation of the nephric duct was previously reported by our laboratory (Grote et al. 2006). However, this early phenotype made it impossible to determine any functions of Gata3 at later stages. In order to overcome this limitation of the *Gata3* null mice a conditional knock out mouse was generated. $Gata3^{flox}$ mice were crossed with $HoxB7^{cre}$ mice. $HoxB7^{cre}$ begins deletion at E9.0 allowing the early phenotype to be bypassed. The resulting mice displayed hydronephrosis, megaureter, and blunt ended ureters that did not connect to the bladder. Further examination of these mice at earlier stages revealed delayed extension of the nephric duct and failure to fuse with the cloaca by embryonic day E10.5. Additionally we found that there were far fewer cell extensions at the tip of the nephric duct in the *Gata3* conditional mutants than in wild type mice (Figure 8).

Gata3, *Ret* and Retinoic Acid

Interestingly, Ian Chia and Cathy Mendehlson had discovered that *Ret* null mice that did not display kidney agenesis and *Raldh2* null mice displayed hydronephrosis and blunt ending ureters, which was strikingly similar to what was observed in our Gata3 null mice. Thus we chose to examine the genetic interactions between *Gata3, Ret* and *Raldh2* by *in-situ* hybridization.

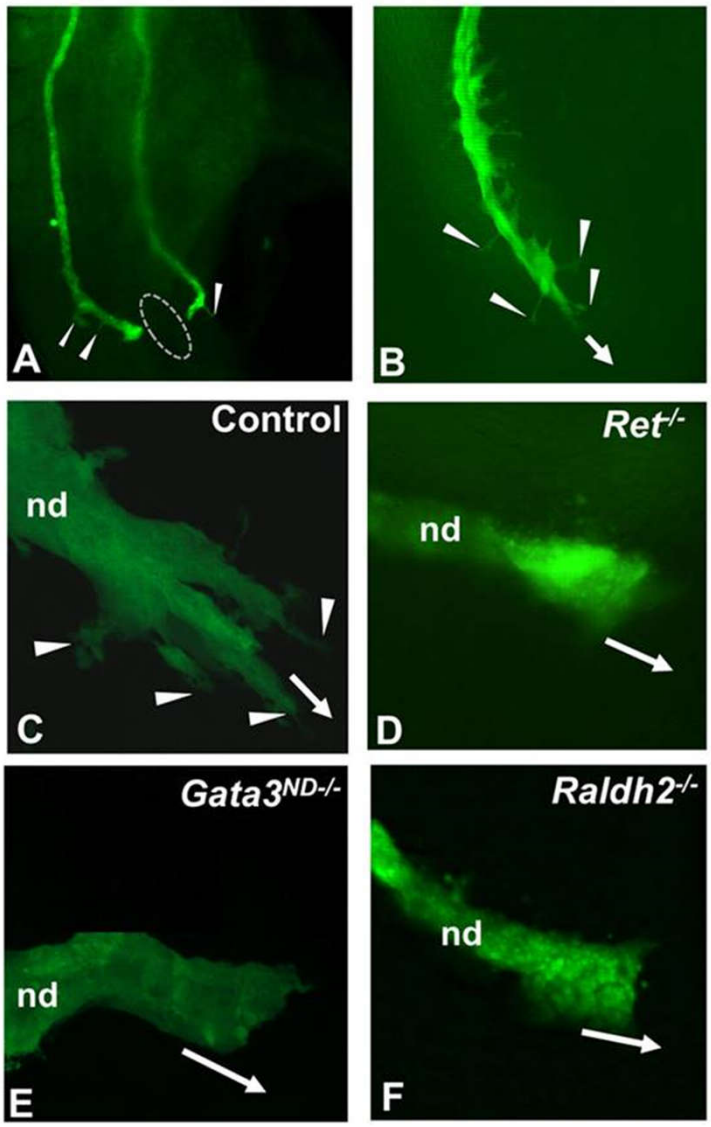

Chia I et al. Development 2011;138:2089-2097

Figure 8. Wild-type Embryos Display Prominent Extensions that are not Visible in *Ret*, *Gata3* or *Raldh2* Mutant Embryos. (**A**) A whole-mount wild-type *Hoxb7-Gfp* embryo at E9.5 showing nephric ducts (NDs) that have extended and migrated to the cloaca (dashed oval). Cellular extensions are visible in the more posterior segment (arrowheads). (**B**) Higher magnification image showing posterior cellular extensions in a control *Hoxb7-Gfp* embryo (arrowheads). (**C**) High magnification image showing cellular extensions (arrowheads) at the tip of a E9.5 *Hoxb7-Gfp* control nephric duct. (**D**) Absence of visible ND extensions in *Hoxb7-Gfp*;*Ret* mutant at E9.5. (**E**) Absence of visible GFP-positive ND extensions in *Gata3*$^{ND-/-}$ mutant embryo at E9.5. (**F**) Absence of ND extensions in E9.5 *Raldh2* mutant embryo. White arrows in B-F denote the direction of growth. nd, nephric ducts. Magnifications: 10× in A; 12× in B; 40× in D-F.

In *Gata3* mutants, we found reduced levels of *Ret* but *Raldh2* levels were unaltered. While in *Raldh2* mutants, *Ret* levels were reduced but *Gata3* levels were unaffected. Thus both Gata3 and Raldh2 were independently required for the expression of Ret in the nephric duct (Figure 9). Interestingly, it was shown by our collaborators that *Ret* mutants, like *Gata3* mutants, displayed delayed duct elongation and a reduced number of cell extensions at the duct tip. These findings suggest that the cell extensions play an important role in duct elongation and fusion with the cloaca and that Ret is likely a key regulator of the formation of these extensions and expression of Ret is regulated in turn by Gata3 and Raldh2.

These filopodia like extensions at tip of the nephric duct were reported in axolotl as early as 1982 (Poole & Steinberg 1982). The presence of filopodia suggests that guided active migration occurs in nephric duct development. However, static images of these extensions revealed little information about the role they may play in nephric duct development. These observations were among those that prompted us to develop the live imaging techniques described in chapter III.

In static images we have observed lateral extension coming off of the side of the nephric duct, sometimes quite far from the tip. Time lapse imaging revealed that most lateral extensions formed at the tip then persisted in place and acquired lateral positioning as the migration front moved forward. Some lateral extensions also emerged from the side of the duct away from the tip. However, all of these extensions were short lived and most retracted into the duct shortly after emerging. Live imaging analyses showed no extensions of any significant length or any that persisted for a significant amount of time formed from the side of the nephric duct.

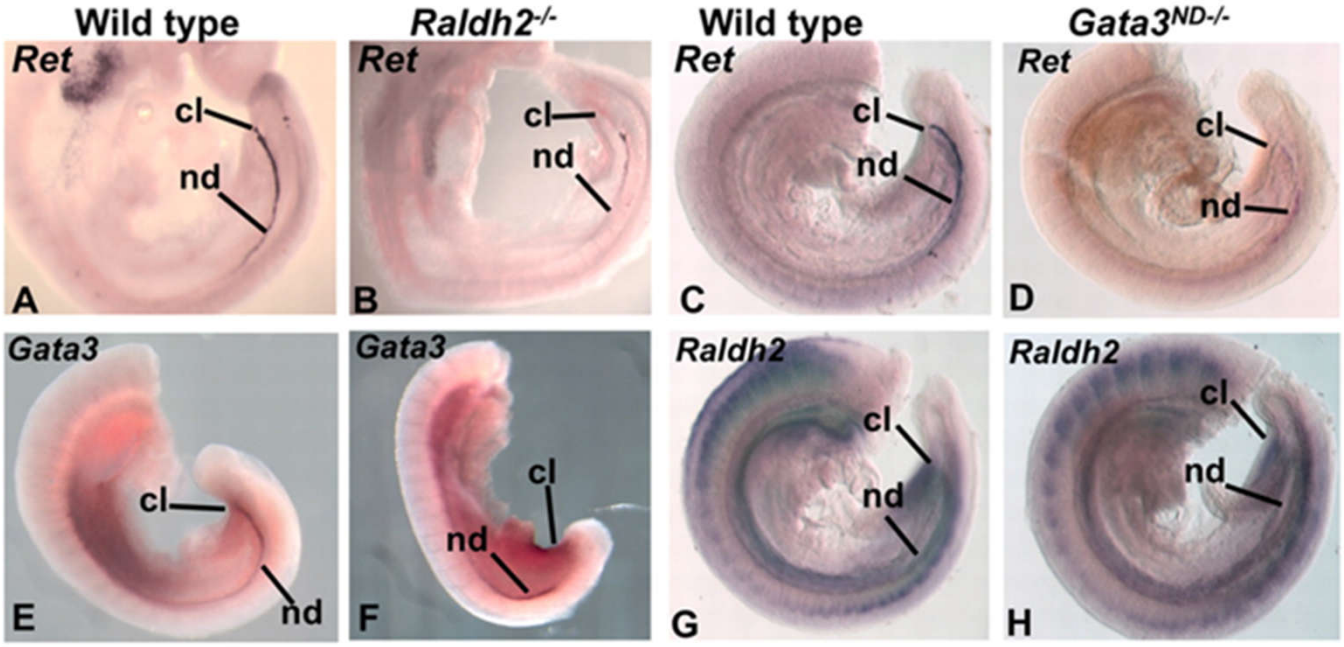

Figure 9. Retinoids and Gata3 act in Parallel to Regulate Ret Expression in the Mouse Nephric Duct (ND). (A) Ret expression in the nephric ducts of a whole-mount E9.5 wild-type embryo. (B) In situ hybridization analysis of an E9.5 Raldh2−/− mutant embryo showing down-regulation of Ret in the ND, which has terminated prematurely. (C) Whole-mount in situ hybridization analysis of an E9.5 wild-type embryo hybridized with Ret probe. (D) Down-regulation of Ret in an E9.5 whole-mount Gata3ND−/− mutant. (E) Gata3 expression in a wild-type E9.5 embryo. (F) Gata3 expression in an E9.5 Raldh2−/− embryo. (G,H) Raldh2 expression in control (G) and in a Gata3ND−/− mutant embryo (H). cl, cloaca; nd, nephric duct. Magnifications: ×20 in all panels.

However, it is still possible that lateral extensions that form on the side of the duct may extend further from the nephric duct or persist for longer. It is also unclear whether these extensions have a functional role.

Another exciting finding from our imaging is that the region of the duct trailing the tip becomes significantly thinner over time, confirming in mice what had previously been reported in the axolotl (Poole & Steinberg 1981). This indicates that there is cell rearrangement occurring in the nephric duct. Along with this we have observed the active migration of cells within the nephric duct moving towards the tip (Supplementary Video 2). It has been difficult to track individual cells in the $Pax2^{GFP}$ mice. However, it is visually apparent that there are motile cells within the stalk of the nephric duct and that these cells are moving in the direction of duct elongation. What is observed is consistent with cell rearrangement and a convergence extension type mechanism. Although the cell behavior is difficult to observe in the videos obtained, neither mediolateral intercalation nor rosette formation accurately describe the apparent phenomenon. Rather there is a migration of cells towards the tip of the nephric duct, which may be accompanied by a convergence movement. This may also result in the convergence of the cells at the exterior after interior cells vacate the region.

Model of Collective Cell Migration in the Nephric Duct

It is also likely that motile stalk cells overtake the tip after these tips cells stabilize cells and become the new leader cells. Time lapse imaging of the nephric duct *in-vivo* revealed that these extensions are highly active (Figure 10, Supplementary Video 1).

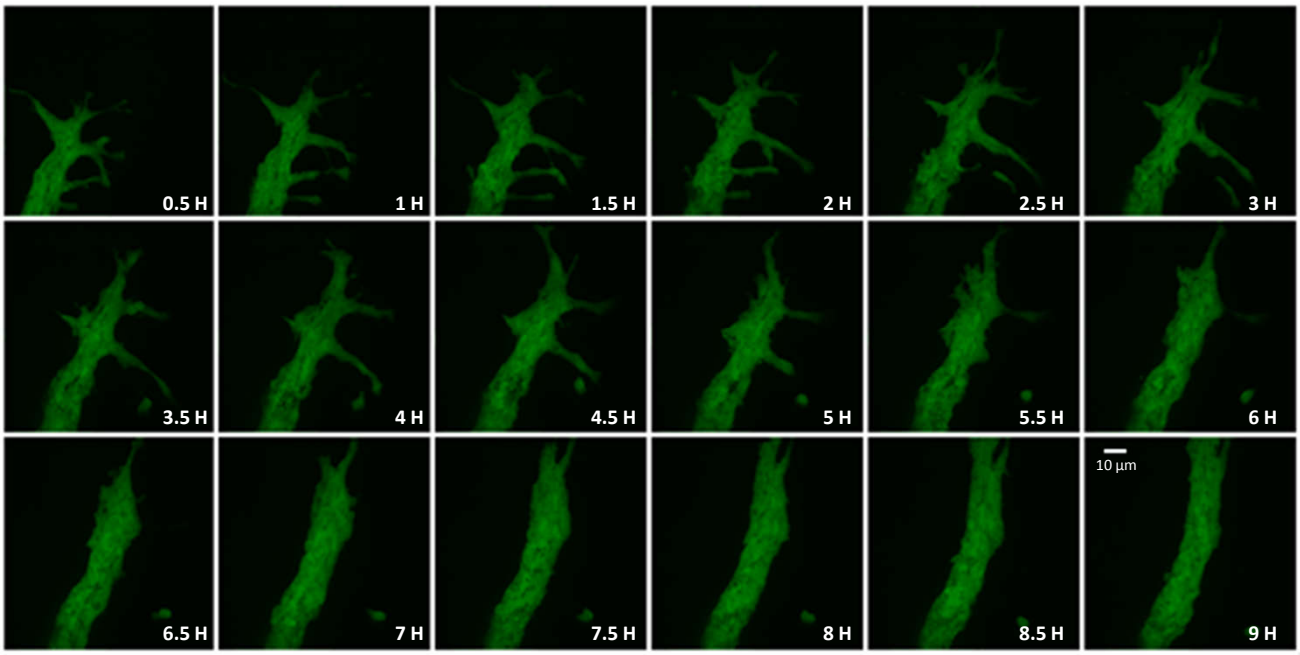

Figure 10. Nephric Duct Cell Extensions are Highly Active
This montage shows the highly active cell extensions of the nephric duct over approximately 9 hours.

Analysis of the videos obtained of nephric duct has revealed an apparent pattern of behavior at the tip of the nephric duct. These observations have been made in multiple movies at various stages of development. This pattern suggests a possible model of duct growth which proceeds through the following series of steps. First the nephric duct sends out filopodia like extensions forward and laterally. These extensions sense the surroundingenvironment and stabilize or retract depending on the signaling encountered in the surrounding environment. The extensions that receive the correct signaling will stabilize and those cells will migrate towards the signal forming long thin extensions while maintaining a connection to the nephric duct. Cells from the stalk of the nephric duct then migrate forward following this first extension. Once the tip is replenished, a new round of extensions begins to form and the process repeats (Figure 11).

This model of elongation may be the result of a cyclical process occurring near the migration front, such as the segmentation clock. This behavior maybe in response to a cyclical signal or may be a product of repetitive structural elements, namely the somites. Alternatively, this behavior could be intrinsic to the duct resulting from a network of paracrine, autocrine and juxtacrine signals.

Imaging at early stages of development revealed a different pattern of behavior. Where nephric duct cells which strongly expressing GFP were observed form short filopodia and to migrate collectively over cells weakly expressing GFP. The cells that have weak GFP expression are likely cells in the nephric cord which is known to weakly express Pax2 and in our mice GFP is expressed from the Pax2 locus. (Grote et al. 2006)

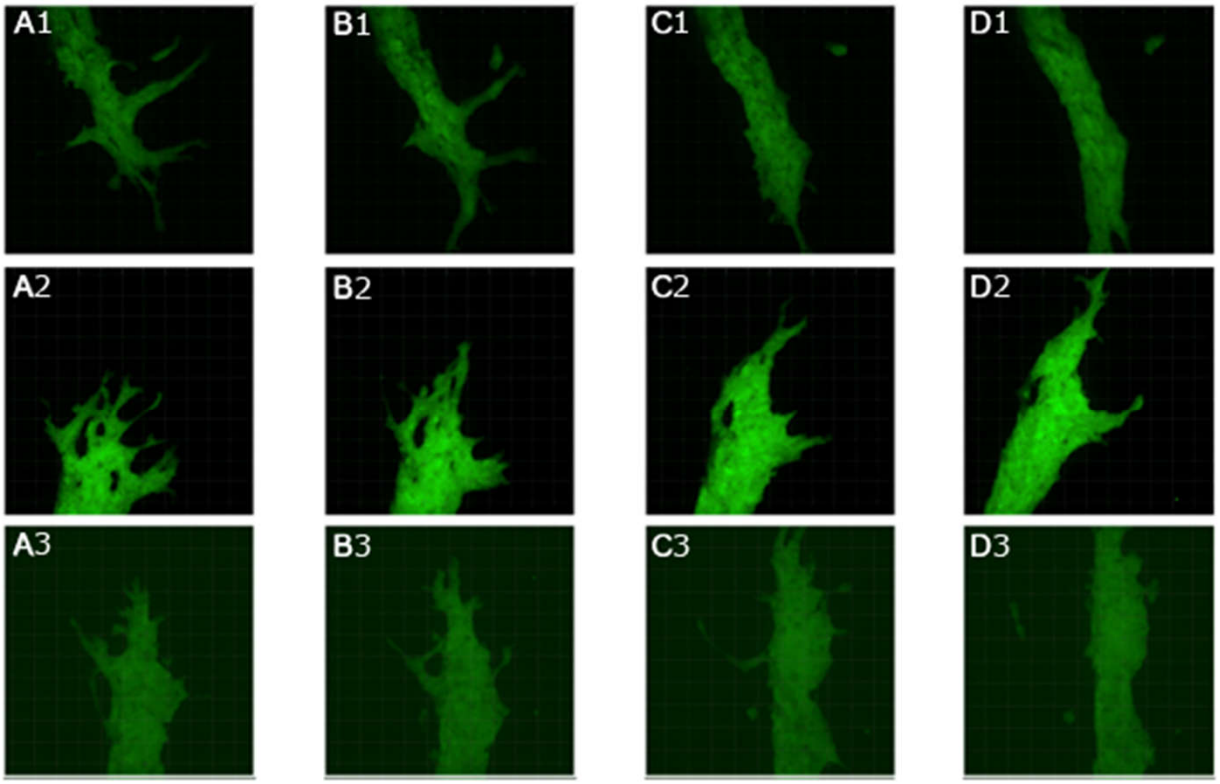

Figure 11. Cyclical Model of Nephric Duct Elongation.
We propose a model of nephric duct morphogenesis where tip cells first explore the surrounding environment presumably searching for a guidance signal **(A1, A2, A3)** . Then the tip cells migrate in the direction of the signal **(B1, B2, B3)**, the tip cells which encounter high levels of signal form stable contact with the extracellular matrix, other cell extensions retract into the duct **(C1, C2, C3)**, migratory stalk cells overtake the now ECM stabilized tip cells and become the new tip cells **(D1, D2, D3)**.

The cell behavior displayed by these cells also differs from what was observed at later stages as long cell extensions were not observed. Once the migration front bypasses the point of the weakly expressing GFP cells the behavior of the cells becomes reminiscent of the later stages of development. Perhaps this behavior appears similar to the collective cell migration that is occurring behind the tip at later stages.

Screen for Guidance Molecules

The presence of these filopodia like cell extensions suggests that there is some morphogen signal that is being followed by the duct. To identify potential guidance signals that may mediate this effect, a broad candidate screen was initiated. A list of candidate genes was compiled based on an extensive literature search for potential morphogens. Each was assessed for expression in the posterior region between E8.5 and E14.5 on *in-situ* hybridization in the GUDMAP (gudmap.org/index.html) and Emage (www.emouseatlas.org/emage/home.php) gene expression databases and on microarray data from GUDMAP (McMahon et al. 2008; Richardson et al. 2014). Candidate genes were initially selected based on expression analysis by *in-situ* in the kidney, ureter, bladder or surrounding tissue. As well as by microarray expression in the E11.5 nephric duct, metanephric mesenchyme, uretric bud, E10 ureteric tip and ureteric trunk, E13.5 bladder. From the initial list, expression at E9.5 was assessed by semi-quantitative PCR. Each candidate was classified as negative for expression, present or strongly expressed. This still left 82 genes expressed in the tail region at E9.5. (Table 1) This was the first step towards identifying the morphogen responsible for nephric duct guidance. It has since been identified that

FGFs likely play a major role in nephric duct guidance. In chick that Fgf8 is able to chemoattract the nephric duct and that inhibition of Fgf signaling halts nephric duct progression (Atsuta & Takahashi 2015; Attia et al. 2015). However, it is likely that additional guidance signals are involved in nephric duct migration. Indeed, Fgf8 gradient is unidirectional leading to tail bud, however the nephric duct must turn to fuse with the cloaca. In addition, the nephric duct stays in contact with the lateral plate mesoderm. As the Fgf gradient is roughly even

across any ventral cross-section of the intermediate mesoderm this gradient alone would be unlikely to be able to keep the nephric duct in contact with the lateral plate mesoderm. As such this screen may still prove useful, to look for additional guidance cues. Several of these genes have been implicated in budding and or branching including Fgfs, Semaphorins, Angiopoietin, Bmps, Wnts. Other interesting candidates are Ephrins, Tgf, Egf and Vegf. A potential follow up experiment would be to verify the expression of receptors for these candidate genes by qPCR on nephric duct cells sorted by flow cytometry. Additional experiments would be to use blocking antibodies, agonists or inhibitors against the receptors of the best candidates in embryo culture experiments. The best candidates would be receptor-ligand pairs that have the receptor expressed in the nephric duct and ligand expressed in the surrounding mesenchyme.

No expression in UGS (Gudmap)			Positive for expression in GUDMAP						
			Not detected by PCR		Low	Moderate		High	
Artn	Fgf3	Itgb7	ar	nrp2	Bmp8b	BDNF	sema3g	angpt1	ptn
Bmp1	Fgf4	Itgb8	Btc	nrtn1	itgb3	Bmp10	sema4a	angpt2	sema3b
Bmp3	Fgf7	Notch2	Efna1	pigf	fgf20	bmp2	sema4b	anln	sema3e
Efna2	Gdf6	Nrg2	Egf	plxnb2	Sema3c	Bmp8a	sema4c	bmp1	sept2
Efna3	Gdf8	Nrp1	Epgn	prox1	sema4f	egf	sema4g	Bmp15	slit1
Efna4	Gdf9	Ntn3	fgf1	robo1	shh	Epha1	sema5b	bmp4	spry1
Efna5	Gremlin	Ntn4	fgf14	sema3d	spred3	ephb4	sema6a	bmp5	tgfb3
Efnb1	HBEGF	Ntn5	Fgf2	sema6b	wnt1	fgf12	slit2	Bmp6	wnt2b
Efnb2	Igf1r	Plgf	fgf22	wnt10a	wnt10	fgf13	slit3	bmp7	wnt3
Efnb3	Inha	Plxna1	fgf23	wnt11	wnt8a	fgf17	sema4d	efna5	wnt5b
Egfr	Inhba	Plxna2	fgf5	wnt6		fgf18	spred1	Epha2	wnt7b
Epha10	Inhbb	Plxna4	fgf6	wnt8b		fgfr4	spred2	ephb2	
Epha3	Itga1	Plxnb3	gdf1	wnt9a		gdf7	spry2	fgf10	
Epha4	Itga10	Plxnc1	gdf2	wnt9b		gdnf	spry3	fgf8	
Epha5	Itga11	Plxnd1	gdf3			igf1	spry4	fgf9	
Epha6	Itga2	Pspn	gdf5			itga3	tgfa2	fgfr1	
Epha7	Itga4	Sema5a	ihh			nrg1	tgfb1	fgfr2	
Epha8	Itga5	Sema6c	inhbc			ntn1	vegfc	fgfr3	
Ephb1	Itga6	Sema6d	inhbe			plxna3	wnt10b	fgfrl1	
Ephb3	Itga7	Sema7a	itgb2			prox2	wnt16	Ifgr2	
Ephb6	Itga8	Tgfa	notch3			robo2	wnt2	igf2	
Ereg	Itga9	Tgfb2	notch4			secretin	wnt4	notch1	
Fgf11	Itgb1	VegfA	npy			sema3a	wnt5a	nrg4	
Fgf15	Itgb3	VegfB	nrg3			sema3f		plxnb1	
Fgf16	Itgb4	VegfD							
Fgf19	Itgb5	Wnt3a					-		
Fgf21	Itgb6	Wnt7a				-	-		

Table 1. Results of Expression Screen for Candidate Guidance Genes in the Nephric Duct.

Distribution of Mitoses in the Nephric Duct

The role proliferation plays in the elongation of the nephric duct has been a long standing question. There is a consensus that the nephric duct grows via proliferation accompanied by migration and cell rearrangement, rather than cell recruitment. However, there remains questions on the distribution of proliferation, how the rate of proliferation compares to that of the surrounding tissue and the nature of the cell rearrangement accompanying migration. Most of the research to address these questions has been only been done in chick or amphibians such that very little is known of the role of proliferation in nephric duct elongation in the mouse.

It has been reported in chicks that proliferation occurs throughout the duct (Jacob et al. 1992). This is in direct contradiction to previous work also in chicks showing elevated levels of proliferation at the duct tip (Gruenwald 1942; Overton 1959). We examined these questions in the mouse using antibodies against phosphorylated histone 3 to mark proliferative cells in *Pax2*^{GFP} transgenic mice in which the nephric duct expresses GFP. We found that between 4% and 8 % of nephric duct cells were undergoing proliferation at any given time and this proliferation occurred throughout the nephric duct (Figure 12). Our results confirm that in the mouse, proliferation occurs throughout the nephric duct.

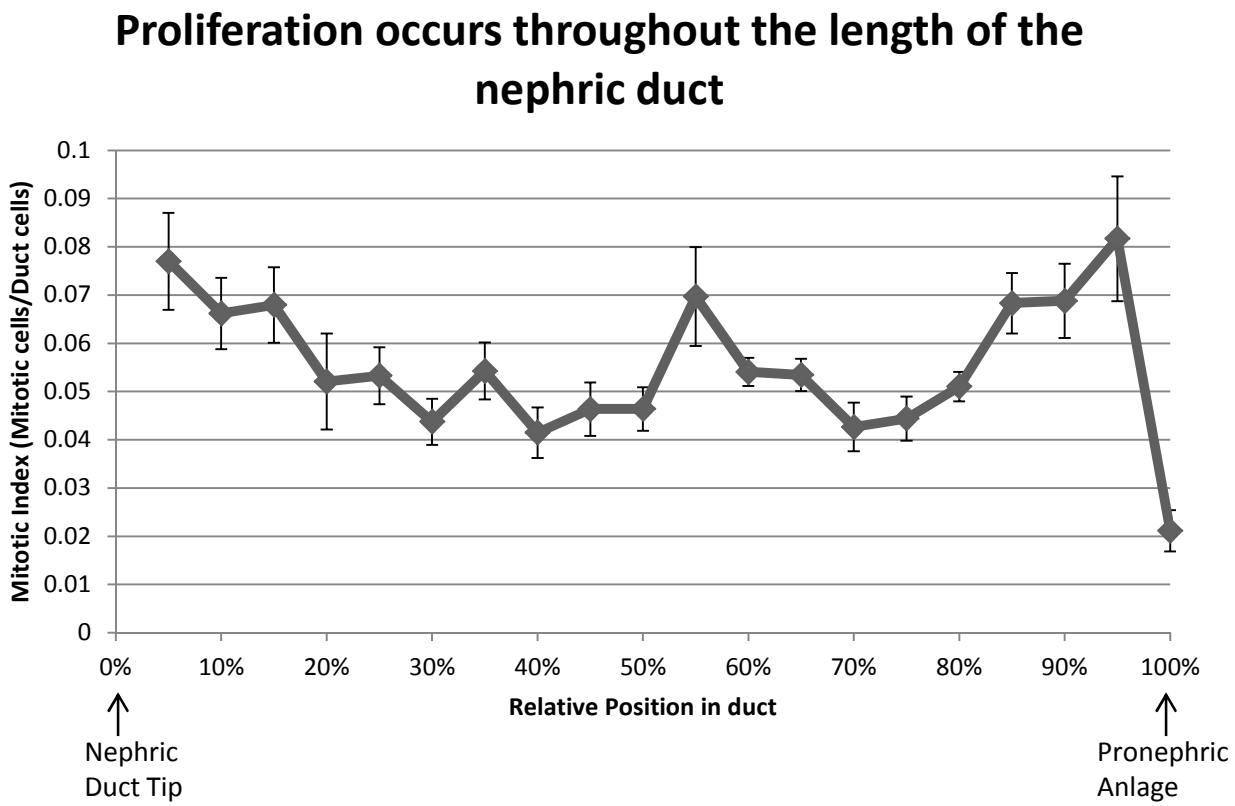

Figure 12. Cell Proliferation Occurs Throughout the Length of the Nephric Duct. Rate of mitosis within each 5% portion of the duct plotted against the relative length of the duct. The rate of mitosis is statistically the same throughout the length of the nephric duct. Error bars represent standard error.

Pattern of Oriented Cell Division in the Nephric Duct

To better understand the contribution of proliferation to nephric duct elongation we imaged cells undergoing mitosis using a marker for mitotic cells. We then determined the angle of mitosis with respect to the axis of elongation. Such measurements were performed throughout the entire length of the duct at different stages of duct development. Before the 20 somite stage, cell divisions were randomly oriented throughout the duct. However, during the 21-25 somite stage the angle of cell division was significantly oriented along the axis of duct elongation in the caudal half of the nephric duct. In the caudal part of the duct the majority of cell divisions were less than 45 degrees from the axis of the duct (with an average angle of division was 30 degrees) (Figure 13), indicating that cell division was indeed oriented with the direction of elongation. This orientation was found to be significant by the Mann-Whitney U-test and by the Kolmogorov-Smirnov test. Within the rostral portion of the duct orientation of cell division was lost. Given that Gata3 mutants displayed an abnormal elongation and proliferation (Grote et al. 2006) we decided to examine the orientation of cell division in mutants for Gata3. Strikingly, we found that the orientation with the axis of elongation was lost in Gata3-deficient cells (Figure 13). From the Kolmogorov-Smirnov test it can be said that the distribution of the angles were drawn from different populations with a D value of 0.5844, and a corresponding P value of less than 0.0005. The Mann-Whitney U-test results in a z score of -3.1173 with a corresponding P value of 0.0009. From these results we conclude that oriented cell division is an integral part of caudal nephric duct extension and that Gata3 is necessary for this process.

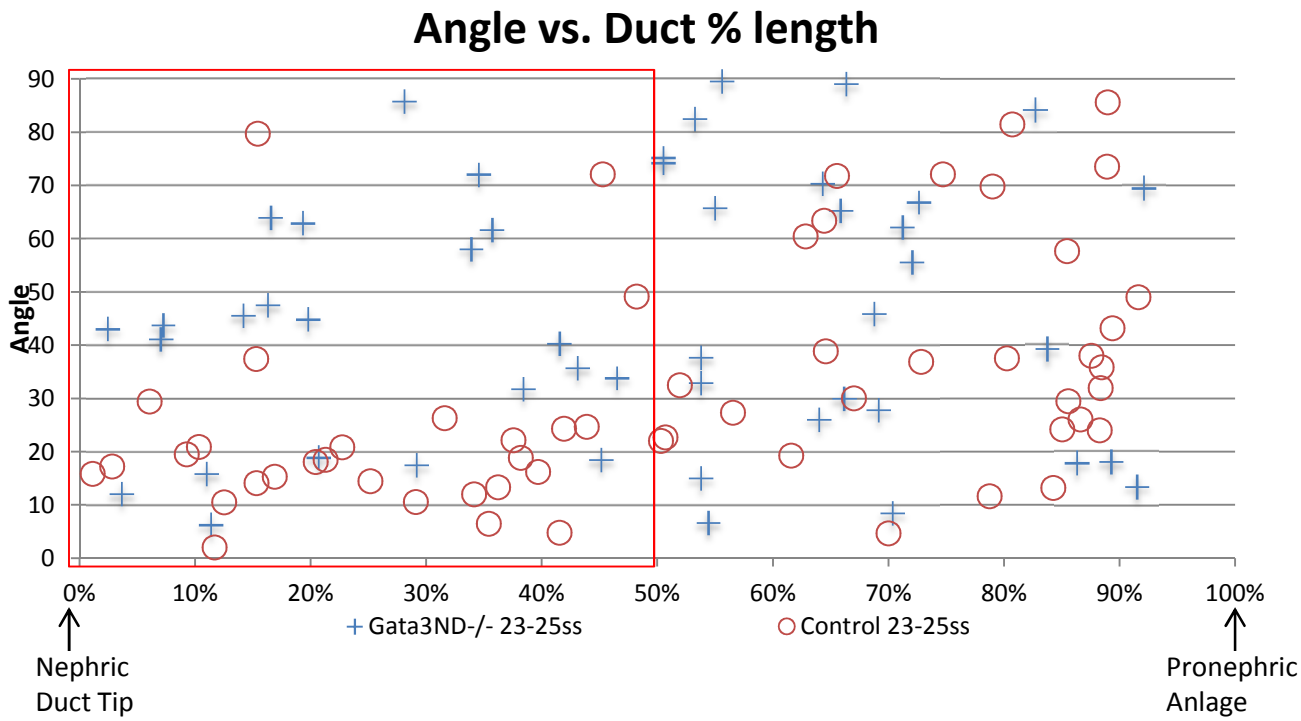

Figure 13. Oriented Cell Division in the Nephric Duct of Wild Type and Gata3 Conditional Knockouts. Cells of the caudal nephric duct orient themselves with the axis of cell elongation (Box, Red circles) but not in the gata3 conditional mutant (Box, blue crosses). The rostral nephric duct does not display oriented cell division.

VANGL2 and GATA3 Do Not Interact Genetically in Kidney Development

The loss of OCD in Gata3 mutant mice could result from a defect in spindle orientation or a deficiency in planar cell polarity. To explore this question, we decided to look at PCP and investigate whether there might be a genetic interaction between *Gata3* and the core PCP protein. A key component of the core PCP pathway is *Vangl2*. Interestingly, *Vangl2* mutant mice have hypoplastic kidneys, and display reduced branching and fewer glomeruli (Yates et al. 2010). To assess whether there was a genetic interaction between these two genes we crossed *Gata3* mutant mice ($Gata3^{GFP}$) mice with *Vangl2* loop tail mice (Strong & Hollander, 1949) provided by our collaborator Dr. Philippe Gros. We first investigated the gross anatomy of the double heterozygotes at E18.5. In three double heterozygote embryos we found no difference in the gross anatomy of the kidney (Figure 14 A-F). The area of each kidney was measured and there was no difference in the overall size of the kidney (Figure 14 G). However, as the *Vangl2* mutant phenotype is mild we decided to generate Gata3 heterozygotes Vangl2 knockouts. These mice had phenotypes consistent with those of Vangl2 homozygous mutants (Figure 14 H). This result suggests an absence of a genetic interaction between Gata3 and Vangl2, and argues that Gata3 regulation of OCD is independent of the core PCP pathway.

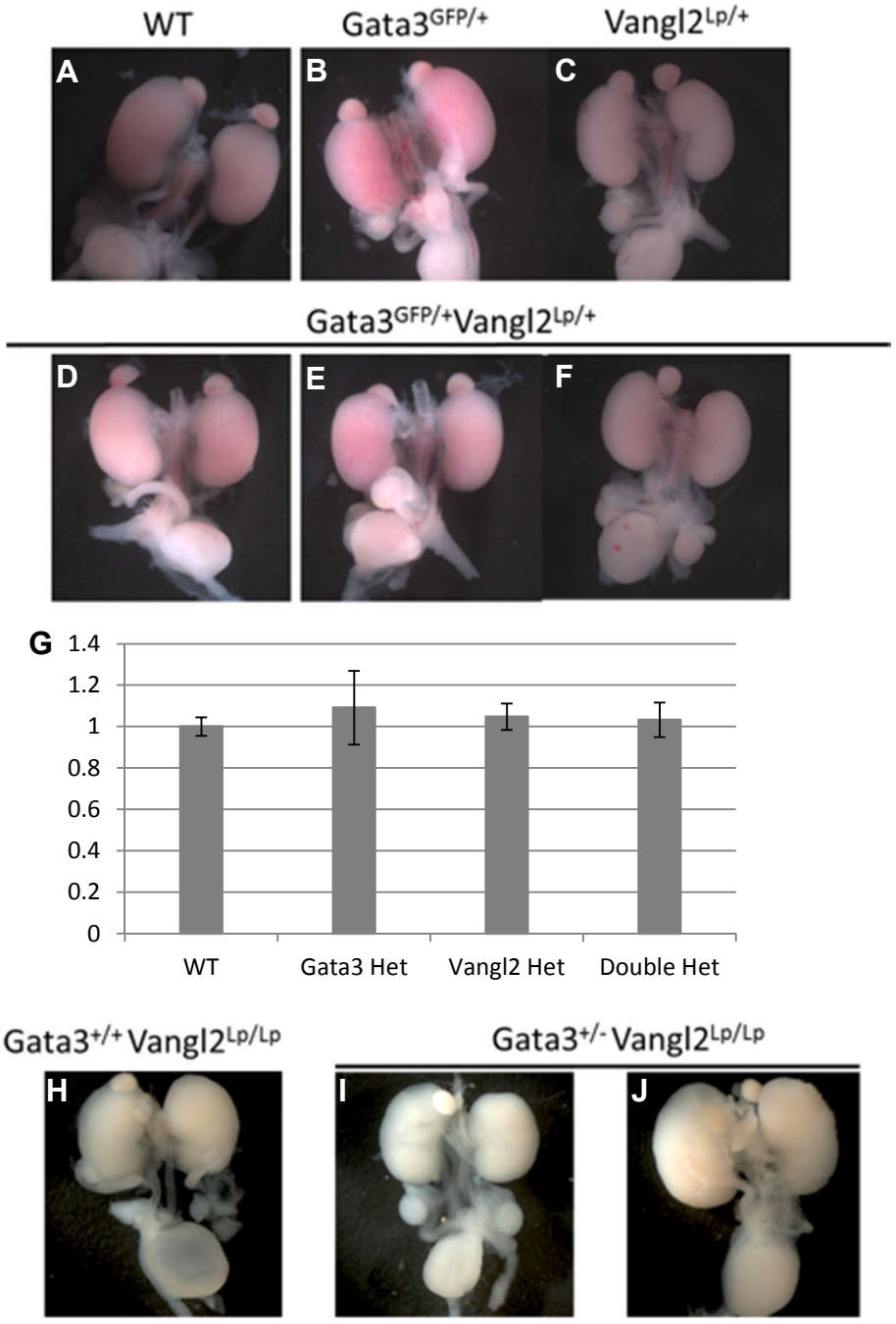

Figure 14. Gata3 and Vangl2 Have no Significant Genetic Interactions. There is no obvious phenotypic difference between wild type kidneys (A, B, C) and Gata3 Vangl2 double heterozygotes (D, E, F). The surface are of the kidneys was examined (G) and normalized to the average size of the Wild type kidneys. The size of Gata3 Vangl2 double heterozygotes kidneys are not significantly different from wild type. No phenotypic difference was found between vangl2 mutant kidneys (H) and Gata3 het Vangl2 mutant Kidneys (I, J)

Chapter V: Discussion

The stated goal of this thesis was to advance our understanding of the mechanism by which the nephric duct elongates to the cloaca. Many questions about this process remain open, however one of the significant contributions is the development of a new technique for the study of nephric duct elongation.

Live imaging

We developed experimental conditions allowing long term live imaging of the developing mouse mesonephros ex-utero. This technique allows for the dynamic processes of development to be examined as they happen. This is an exciting tool that provides a new experimental approach in mouse developmental biology. The technique established by our laboratory described in chapter three and published in (Grote et al. 2012) adds to the knowledgebase of embryo culture techniques and will contribute greatly to the ongoing study of nephric duct development. Specifically this technique has been optimized for longer term imaging of mouse mesonephros than previous techniques have been capable. Furthermore the publication of this technique marks one of the most complete methods papers describing a live imaging technique in mouse embryos. It contains extensive notation as well detailed advice, which would often be omitted from a typical methods paper. A potential issue with this technique is the question of how accurately does ex-vivo development represent in-utero development. This is an issue faced by many new techniques, especially those involving tissue culture. One method of assessing how well ex-utero development reflects in utero development is to compare the state of development of an embryo after ex-utero culture to an embryo at a similar stage. For the initial few hours of development these differences seem to be minimal.

While over the course of a 24-hour experiment there will be a significant divergence in ex-utero and in-utero development. It seems that this is principally due to a reduction in embryo viability after long-term removal from the uterus. To address any criticisms from this issue, results from very long-term imaging can be complemented with fixed images from precisely staged embryos.

Despite the challenges of live imaging and potential criticism of ex-utero culture, live imaging of embryos allows us to see development happen in a way not previously possible. By combining the dynamic data from living tissue with the expression and localization data available from fixed tissue we can gain a powerful insight into how the animal body is formed.

An interesting observation emerging from our live imaging of mesonephros is the observation of cellular extensions at the growing tip of the duct. These filopodia, discussed in chapters III and IV, were first observed in Axolotl in 1982 (Poole & Steinberg 1982) and were reported again by us in mice (Chia et al. 2011). These filopodia were highly dynamic further cementing the idea that chemoattractive guidance was an important mechanism for the elongation of the nephric duct (Supplementary Video 3).

During the writing of this thesis it has been published that Fgf8 is indeed a chemoatractive signal necessary for the ordinary development of the nephric duct (Attia et al. 2015; Atsuta & Takahashi 2015). This Fgf8 gradient provides a means for the nephric duct to elongate through the intermediate mesoderm to the level of the cloaca. However, in order to reach the cloaca the nephric duct must turn approximately perpendicular to this Fgf8 gradient. As such the Fgf8 gradient seems

unlikely to provide a means of guidance to the cloaca itself. It is then likely that a secondary signal causes turning towards the cloaca. Gdnf/Ret is a candidate for such a secondary signal. Gdnf was shown to be responsible for guidance in axolotl (Drawbridge et al. 2000). In mice null for Ret mutants the nephric duct does not fail to elongate but displays an unusual path towards the cloaca and fails to fuse with the cloaca or fusion is delayed (Chia et al. 2011) It may be that Fgf8 drives early elongation of the nephric duct caudally, and turning and fusion with the cloaca requires Gdnf. However, it is possible that more mechanisms of guidance and elongation are present in the nephric duct.

Studies in axolotl suggest that both diffusible and contact driven guidance mechanism are present (Drawbridge et al. 2000; Morris et al. 2003). Whether a contact mediated guidance signal in the mouse is not yet known. However it has been shown that insertion of the nephric duct in the cloaca requires ephrinA4/A7 in the mesenchyme and ephrinB2 in the nephric duct (Weiss et al. 2014). Some of our results also suggest a contact driven mechanism. A video of early nephric duct development shows cells migrating in a manner consistent with contact guided cell migration which contrasts strikingly with the behavior of nephric duct cells at later stages of development (Supplementary video 4). Although only a preliminary result, the observation of motile cells away from the tip of the duct was especially intriguing. Future use of the live imaging techniques would be to characterize in greater detail the behavior of the tip cells as well migratory cells in the duct. Live imaging of the confetti mice, which allows tracking of individual cells by randomly

coloring all cells, will likely give a much clearer image of what is occurring in the stalk of the nephric duct.

Similar behaviors to what we observe have been reported in angiogenesis and vascular development, the “tip cell overtaking” and “cell mixing” behaviors that have been recently observed are especially relevant (Arima et al. 2011; Jakobsson et al. 2010). In this model, tip cells and stalk cells are interchangeable and cells of the branching endothelium are divided in to highly motile and minimally motile cell populations. The highly motile stalk cells compete with and overtake tip cells, becoming the new tip cells. As tip cells have reduced mobility, after a stalk cell overtakes a tip cell, it will slow and be overtaken in turn by other highly motile stalk cells (Jakobsson et al. 2010). In the nephric duct we observe tip cell being highly motile then stabilizing and being overtaken by stalk cells. We also observe highly motile cells within the stalk, which may be evidence of a phenomenon similar to the cell mixing described in angiogenesis.

Another result from our live imaging experiments is our proposed model of nephric duct elongation. This model consists of cyclical pattern of sensing the environment with short filopodia, extending long filopodia in the direction of migration, then the stalk cells following the long filopodia. This pattern has been observed in multiple videos but to better support this model it would desirable to obtain multiple long-term videos showing this pattern of elongation over multiple cycles.

As the primary guiding signal for these extensions is Fgf signaling (Atsuta & Takahashi 2015) it is possible that Fgf is submitted to cyclical waves of activity in the caudal trunk.

Interestingly *in silico* models predict that the tip cell overtaking behaviors could result in cyclical clustering of cells with similar receptor levels (Jakobsson et al. 2010). This is reminiscent of the cyclical model of duct elongation that we have suggested. A future direction of this project would be to characterize this mechanism in detail and validate the proposed model of duct elongation.

Future Directions For Live Imaging

In addition to some of the follow up experiments discussed above there are myriad potential uses for this technique in our laboratory.

Additional experiments comparing mutants and wild type mice will likely be very informative. The primary candidate gene of such an approach would be *Gata3*. It was shown to have elongation and guidance defects and as such it would be interesting to see in live imaging which cellular processes are disrupted. Additionally, other mutants with nephric duct defects available for study in the laboratory are *Pax2* and *Lim1* mice, which could be used to dissect the guidance cue.

A future tool for live imaging would be to cross the $Pax2^{cre}Rosa26^{conf}$ with $H2B^{GFP}$ mice, which express nuclear GFP in all cells. The background fluorescent cells can be used as stationary points of reference allowing more accurate tracking of cells. Such an experiment will also serve to show whether the cells around the nephric duct are static or are dynamically involved in the migratory process.

Analysis of elongation at different stages would also be interesting. One video obtained at shortly after nephric duct induction has revealed a distinct mode of nephric duct cell migration in which the nephric duct cells form very short extensions and seem to navigate via contact mediated guidance cues

(Supplementary Video 4). It would also be insightful to image uncharacterized stages of nephric duct development such as induction of nephric duct cells or fusion of the nephric duct with the cloaca.

Live imaging of the *Pax2* mutant may also be useful in the analysis of nephric duct specification. For example, embryos can be cultured and imaged at E8.5 or earlier and in the presence of inhibitors or activators of pathways of interest, in this way the roles of such pathways in nephric duct induction or maintenance can be dissected.

Culture of embryos in the presence of pathway agonist or antagonist can be a method of elucidating which pathways are contributing to nephric duct growth. Of note, inhibitors of important migratory pathway regulators such as JNK, Ras, ROCK, Rac, Cdc42 have been obtained for such an experiment.

A potentially useful tool for such a project is the primary culture of nephric duct cells which has been developed in the laboratory. If the propagation of such cells becomes feasible it would make a screen for potential molecules much easier. The screen performed in this thesis resulted in many potential morphogens expressed in the posterior region. Other Gdnf family members are among the candidates considered. In the course of this thesis we initiated a screen to identify potential morphogens in the posterior region of the embryo at E9.0, which might act as guidance signals for the nephric duct. Several families of note show up as highly expressed in this screen, FGFs, Wnts, BMPs and semaphorins, which have also been shown to have roles in budding. This screen may be useful as an initial point to begin investigation of potential morphogens, however this screen has several flaws.

Notably the primers were not verified to work for each gene, therefore negative results are inconclusive. Furthermore the number of positive results highlights the fact that the region selected as the portion was simply too large. A useful screen to perform in the future would be to isolate nephric duct cells via cytometric sorting of *Pax2*^{GFP} positive cells, then isolate RNA from these cells and screen for expression of receptors expressed in the nephric duct. One limitation to such an approach is that RNA quantities may be limiting.

Proliferation and Oriented Cell Division in the Nephric Duct

Our results showed proliferation occurs throughout the length of the nephric duct which confirms in mice what was previously shown in chick (Jacob et al. 1992). This also refutes previous reports that proliferation occurs primarily at the tip of the nephric duct and this tip proliferation is what drives nephric duct elongation (Overton 1959).

Perhaps the most interesting result we have observed is the occurrence of oriented cell division within the nephric duct. We observed that cell division in the nephric duct was oriented with the axis of the duct in the caudal most region. We have also observed the disruption of this orientation in mice mutant for *Gata3*, an indication that *Gata3* is important in regulating OCD in the nephric duct.

It is possible that OCD is a driving force of elongation however: it is also possible that cell division orientation is a response to other forces that are contributing to elongation. Interestingly, we have only observed oriented cell division at the latest stages of elongation and only in the caudal portion of the nephric duct. This would be consistent with OCD playing a role only in late development. There may be a

distinct mechanism of elongation only present during the latest part of extension. This may correspond to the period of time when the nephric duct turns away from the somites towards the cloaca. Interestingly in the *Gata3* conditional mutants, and *Ret* and *Raldh2* mutants as the nephric duct seems to extend relatively normally before this turning away from the somites, and when wild type and mutant duct are compared there seems to be a difference in the way in which the duct has turned to face the cloaca. Whether Ret or other morphogens are tied to polarity in the nephric duct remains to be seen. It is also important to note that the rostral portion of the nephric duct at this point is undergoing mesonephric tubulogenesis, which may be why OCD is lost in this section. As such cells of this section would no longer be contributing to the forward growth of the nephric duct. It is also possible that cells of the mesonephric tubules which do not orient with the direction of growth were counted with the mitotic cells of the duct. However, as mesonephric tubule cells express significantly lower levels of GFP this possibility is unlikely. The pronephric anlage is also present at the rostral-most portion of the duct and its morphogenesis is apparently distinct from that of the rest of the nephric duct. This may also represent reasons why orientation of cell division in the duct displays the observed pattern.

Additionally, we have observed that *Gata3* is necessary for the orientation of cell division in the nephric duct. The loss of OCD in Gata3-deficient nephric duct suggests that this is a regulated process during duct elongation and not simply a consequence of directed cell migration that could align mitosis events in the axis of migration. According to Hertwig's rule cells usually divide along their long axis

(Hertwig & Hertwig 1884), as such it would be interesting to examine the orientation of the long axis of nephric duct cells and see if this orients with the axis of duct elongation. We could then examine whether any orientation of the cell's long axes are disrupted in *Gata3* mutants. Two obvious ways *Gata3* may have this effect is by either affecting the planar cell polarity within the duct, or affecting the ability of the mitotic spindle to orient. In the future it would be interesting to examine expression of PCP and spindle orientation genes in *Gata3* mutants. In the *Gata3* null mice, the nephric duct becomes enlarged and hyper proliferative (Grote et al. 2006). Though OCD was only observed at later stages of elongation very early stages were not examined. It may be that failure of cells to orient properly may contribute to the enlarged nephric duct primordium.

Interestingly, spindle orientation genes *Numb* and *Lis1* have both been shown to be down-regulated in a microarray (David Grote unpublished results) comparing levels of RNA isolated from the nephric duct in *Gata3* mutants to wild type mice. This suggests a link between *Gata3* and spindle orientation. An important future experiment for this project would be to validate these results via *in-situ* hybridization or microarray.

Polarity in the Nephric Duct

Several aspects of duct elongation suggest a role for planar cell polarity such as our results with oriented cell division. Another is the likeliness of the presence of cell rearrangement. Both these process would require the directional information that could be provided by PCP. The fact that OCD is disrupted in *Gata3* conditional knockouts raises the possibility that *Gata3* regulates PCP.

Surprisingly, however, our results found no genetic interaction between *Vangl2* and *Gata3*. It may be possible that *Vangl1* may be compensating for loss of *Vangl2*. Hence, additional reduction of Vangl gene dosage by removal of alleles of *Vangl1* may be necessary to uncover a genetic interaction. Though *Vangl1* has no reported kidney phenotype, it is expressed in the mesonephric duct at E9.5 (Torban et al. 2008). If an interaction with the PCP pathway and *Gata3* exists it is possible that *Gata3* interacts with other branches of the PCP pathway, such as the Fat pathway. Crossing *Gata3* mutants with other mutants such as *Fat4* mutants could determine whether there is an interaction between these genes.

Ultimately the goal of this project was to advance the understanding of how the nephric duct elongates. A significant contribution towards this goal was the development of the live imaging techniques. Hopefully this technique will continue to be a powerful tool in our and in many other labs as well. We also addressed some questions with regards to nephric duct elongation that could form the basis of further research in the future. One such example is the role of oriented cell division and its regulation by Gata3. This is an exciting result that hopefully follow up experiments will confirm these results and find the link between Gata3 and OCD. While many questions have remained unaddressed or have been answered by other labs, we feel that the contributions made here significantly advance our understanding of nephric duct elongation mechanisms and epithelial cell biology in vivo.

Bibliography

Arima, S. et al., 2011. Angiogenic morphogenesis driven by dynamic and heterogeneous collective endothelial cell movement. *Development (Cambridge, England)*, 138(21), pp.4763–76. Available at: http://www.ncbi.nlm.nih.gov/pubmed/21965612 [Accessed August 21, 2015].

Atsuta, Y. & Takahashi, Y., 2015. FGF8 coordinates tissue elongation and cell epithelialization during early kidney tubulogenesis. *Development (Cambridge, England)*, 142(13), pp.2329–37. Available at: http://www.ncbi.nlm.nih.gov/pubmed/26130757 [Accessed August 21, 2015].

Attia, L. et al., 2015. Collective cell migration of the nephric duct requires FGF signaling. *Developmental dynamics : an official publication of the American Association of Anatomists*, 244(2), pp.157–67. Available at: http://www.ncbi.nlm.nih.gov/pubmed/25516335 [Accessed February 8, 2016].

Attia, L., Yelin, R. & Schultheiss, T.M., 2012. Analysis of nephric duct specification in the avian embryo. *Development (Cambridge, England)*, 139(22), pp.4143–51. Available at: http://www.pubmedcentral.nih.gov/articlerender.fcgi?artid=3478684&tool=pmcentrez&rendertype=abstract [Accessed August 21, 2015].

Barak, H. et al., 2005. Cell fate specification along the anterior-posterior axis of the intermediate mesoderm. *Developmental dynamics : an official publication of the American Association of Anatomists*, 232(4), pp.901–14. Available at: http://www.ncbi.nlm.nih.gov/pubmed/15759277 [Accessed August 21, 2015].

Barak, H. et al., 2012. FGF9 and FGF20 maintain the stemness of nephron progenitors in mice and man. *Developmental cell*, 22(6), pp.1191–207. Available at: http://www.pubmedcentral.nih.gov/articlerender.fcgi?artid=3376351&tool=pmcentrez&rendertype=abstract [Accessed August 27, 2015].

Barnes, J.D. et al., 1994. Embryonic expression of Lim-1, the mouse homolog of Xenopus Xlim-1, suggests a role in lateral mesoderm differentiation and neurogenesis. *Developmental biology*, 161(1), pp.168–78. Available at: http://www.ncbi.nlm.nih.gov/pubmed/7904966 [Accessed August 21, 2015].

Basson, M.A. et al., 2005. Sprouty1 is a critical regulator of GDNF/RET-mediated kidney induction. *Developmental cell*, 8(2), pp.229–39. Available at: http://www.ncbi.nlm.nih.gov/pubmed/15691764 [Accessed August 21, 2015].

Batourina, E. et al., 2001. Vitamin A controls epithelial/mesenchymal interactions through Ret expression. *Nature genetics*, 27(1), pp.74–8. Available at: http://www.ncbi.nlm.nih.gov/pubmed/11138002 [Accessed August 21, 2015].

Bingham, C. & Hattersley, A.T., 2004. Renal cysts and diabetes syndrome resulting

from mutations in hepatocyte nuclear factor-1beta. *Nephrology, dialysis, transplantation : official publication of the European Dialysis and Transplant Association - European Renal Association*, 19(11), pp.2703–8. Available at: http://www.ncbi.nlm.nih.gov/pubmed/15496559 [Accessed August 21, 2015].

Boualia, S.K. et al., 2013. A core transcriptional network composed of Pax2/8, Gata3 and Lim1 regulates key players of pro/mesonephros morphogenesis. *Developmental biology*, 382(2), pp.555–66. Available at: http://www.ncbi.nlm.nih.gov/pubmed/23920117 [Accessed July 31, 2015].

Bouchard, M. et al., 2002. Nephric lineage specification by Pax2 and Pax8. *Genes & development*, 16(22), pp.2958–70. Available at: http://www.pubmedcentral.nih.gov/articlerender.fcgi?artid=187478&tool=pmcentrez&rendertype=abstract [Accessed August 21, 2015].

Bouchard, M., Souabni, A. & Busslinger, M., 2004. Tissue-specific expression of cre recombinase from the Pax8 locus. *Genesis (New York, N.Y. : 2000)*, 38(3), pp.105–9. Available at: http://www.ncbi.nlm.nih.gov/pubmed/15048807 [Accessed January 14, 2016].

Bulum, B. et al., 2013. High frequency of kidney and urinary tract anomalies in asymptomatic first-degree relatives of patients with CAKUT. *Pediatric nephrology (Berlin, Germany)*, 28(11), pp.2143–7. Available at: http://www.ncbi.nlm.nih.gov/pubmed/23812353 [Accessed August 21, 2015].

Chia, I. et al., 2011. Nephric duct insertion is a crucial step in urinary tract maturation that is regulated by a Gata3-Raldh2-Ret molecular network in mice. *Development (Cambridge, England)*, 138(10), pp.2089–97. Available at: http://www.pubmedcentral.nih.gov/articlerender.fcgi?artid=3082308&tool=pmcentrez&rendertype=abstract [Accessed July 31, 2015].

Choi, Y. et al., 2009. Neuropeptide Y functions as a facilitator of GDNF-induced budding of the Wolffian duct. *Development (Cambridge, England)*, 136(24), pp.4213–24. Available at: http://www.pubmedcentral.nih.gov/articlerender.fcgi?artid=2781055&tool=pmcentrez&rendertype=abstract [Accessed August 21, 2015].

Costantini, F. & Kopan, R., 2010. Patterning a complex organ: branching morphogenesis and nephron segmentation in kidney development. *Developmental cell*, 18(5), pp.698–712. Available at: http://www.pubmedcentral.nih.gov/articlerender.fcgi?artid=2883254&tool=pmcentrez&rendertype=abstract [Accessed February 8, 2016].

Dobrovolskaia-Zavadskaia, N., 1927. Sur la mortification spontanee de la chez la souris nouveau-nee et sur l'existence d'un caractere (facteur) hereditaire, non-viable. *Crit Rev Soc Biol*, (1927), pp.114–116.

Dolk, H., Loane, M. & Garne, E., 2010. The prevalence of congenital anomalies in Europe. *Advances in experimental medicine and biology*, 686, pp.349–64. Available at: http://www.ncbi.nlm.nih.gov/pubmed/20824455 [Accessed

August 21, 2015].

Drawbridge, J., Meighan, C.M. & Mitchell, E.A., 2000. GDNF and GFRalpha-1 are components of the axolotl pronephric duct guidance system. *Developmental biology*, 228(1), pp.116–24. Available at: http://www.ncbi.nlm.nih.gov/pubmed/11087631 [Accessed October 31, 2015].

Dressler, G.R. et al., 1990. Pax2, a new murine paired-box-containing gene and its expression in the developing excretory system. *Development (Cambridge, England)*, 109(4), pp.787–95. Available at: http://www.ncbi.nlm.nih.gov/pubmed/1977574 [Accessed August 21, 2015].

Dressler, G.R., 2006. The cellular basis of kidney development. *Annual review of cell and developmental biology*, 22, pp.509–29. Available at: http://www.annualreviews.org/doi/full/10.1146/annurev.cellbio.22.010305.104340 [Accessed January 6, 2016].

Van Esch, H. et al., 2000. GATA3 haplo-insufficiency causes human HDR syndrome. *Nature*, 406(6794), pp.419–22. Available at: http://www.ncbi.nlm.nih.gov/pubmed/10935639 [Accessed August 21, 2015].

Esquela, A.F. & Lee, S.-J., 2003. Regulation of metanephric kidney development by growth/differentiation factor 11. *Developmental biology*, 257(2), pp.356–70. Available at: http://www.ncbi.nlm.nih.gov/pubmed/12729564 [Accessed August 21, 2015].

Fleming, B.M. et al., 2013. A role for Vg1/Nodal signaling in specification of the intermediate mesoderm. *Development (Cambridge, England)*, 140(8), pp.1819–29. Available at: http://www.pubmedcentral.nih.gov/articlerender.fcgi?artid=3621495&tool=pmcentrez&rendertype=abstract [Accessed August 21, 2015].

Friedl, P. & Gilmour, D., 2009. Collective cell migration in morphogenesis, regeneration and cancer. *Nature reviews. Molecular cell biology*, 10(7), pp.445–57. Available at: http://dx.doi.org/10.1038/nrm2720 [Accessed July 10, 2014].

Fujii, T. et al., 1994. Expression patterns of the murine LIM class homeobox gene lim1 in the developing brain and excretory system. *Developmental dynamics : an official publication of the American Association of Anatomists*, 199(1), pp.73–83. Available at: http://www.ncbi.nlm.nih.gov/pubmed/7909459 [Accessed August 21, 2015].

Gerber, S.D. et al., 2009. The murine Fgfrl1 receptor is essential for the development of the metanephric kidney. *Developmental biology*, 335(1), pp.106–19. Available at: http://www.ncbi.nlm.nih.gov/pubmed/19715689 [Accessed August 27, 2015].

Gong, K.-Q. et al., 2007. A Hox-Eya-Pax complex regulates early kidney developmental gene expression. *Molecular and cellular biology*, 27(21), pp.7661–8. Available at:

http://www.pubmedcentral.nih.gov/articlerender.fcgi?artid=2169072&tool=pmcentrez&rendertype=abstract [Accessed August 21, 2015].

Grieshammer, U. et al., 2004. SLIT2-mediated ROBO2 signaling restricts kidney induction to a single site. *Developmental cell*, 6(5), pp.709–17. Available at: http://www.ncbi.nlm.nih.gov/pubmed/15130495 [Accessed August 21, 2015].

Grote, D. et al., 2008. Gata3 acts downstream of beta-catenin signaling to prevent ectopic metanephric kidney induction. *PLoS genetics*, 4(12), p.e1000316. Available at: http://www.pubmedcentral.nih.gov/articlerender.fcgi?artid=2597718&tool=pmcentrez&rendertype=abstract [Accessed August 21, 2015].

Grote, D. et al., 2006. Pax 2/8-regulated Gata 3 expression is necessary for morphogenesis and guidance of the nephric duct in the developing kidney. *Development (Cambridge, England)*, 133(1), pp.53–61. Available at: http://www.ncbi.nlm.nih.gov/pubmed/16319112 [Accessed August 21, 2015].

Grote, D., Marcotte, M. & Bouchard, M., 2012. Live imaging of the developing mouse mesonephros. *Methods in molecular biology (Clifton, N.J.)*, 886, pp.31–43. Available at: http://www.ncbi.nlm.nih.gov/pubmed/22639249 [Accessed August 21, 2015].

Gruenwald, P., 1942. Experiments on distribution and activation of the nephrogenic potency in the embryonic mesenchyme. *Physiological Zoology*. Available at: http://www.jstor.org/stable/30151653?seq=1#page_scan_tab_contents [Accessed October 31, 2015].

Hains, D. et al., 2008. Role of fibroblast growth factor receptor 2 in kidney mesenchyme. *Pediatric research*, 64(6), pp.592–8. Available at: http://www.pubmedcentral.nih.gov/articlerender.fcgi?artid=2647852&tool=pmcentrez&rendertype=abstract [Accessed August 27, 2015].

Hains, D.S. et al., 2010. High incidence of vesicoureteral reflux in mice with Fgfr2 deletion in kidney mesenchyma. *The Journal of urology*, 183(5), pp.2077–84. Available at: http://www.pubmedcentral.nih.gov/articlerender.fcgi?artid=3657704&tool=pmcentrez&rendertype=abstract [Accessed August 27, 2015].

Heller, N. & Brändli, A.W., 1999. Xenopus Pax-2/5/8 orthologues: novel insights into Pax gene evolution and identification of Pax-8 as the earliest marker for otic and pronephric cell lineages. *Developmental genetics*, 24(3-4), pp.208–19. Available at: http://www.ncbi.nlm.nih.gov/pubmed/10322629 [Accessed August 21, 2015].

Hertwig, O. & Hertwig, R., 1884. *Untersuchungen zur Morphologie und Physiologie der Zelle: Das Problem der Befruchtung und der Isotropie des Eies, eine Theorie der Vererbung*, Available at: https://books.google.com/books?hl=en&lr=&id=PY4tAQAAMAAJ&oi=fnd&pg=PP8&ots=Qy4ZSO3cRI&sig=UpxLowHO7l0dcg3pmok5MxGpCVU [Accessed

August 12, 2016].

Jacob, M., Jacob, H. & Seifert, R., 1992. On the differentiation and migration of the Wolffian duct in avian embryos. *Formation and Differentiation of Early ….* Available at: http://link.springer.com/chapter/10.1007/978-1-4615-3458-7_7 [Accessed October 31, 2015].

Jacquelin, J., 2011. Regressions et trajectoires 3D. , pp.2–12. Available at: http://www.scribd.com/doc/31477970/Regressions-et-trajectoires-3D#scribd [Accessed August 27, 2015].

Jakobsson, L. et al., 2010. Endothelial cells dynamically compete for the tip cell position during angiogenic sprouting. *Nature cell biology*, 12(10), pp.943–53. Available at: http://www.ncbi.nlm.nih.gov/pubmed/20871601 [Accessed May 25, 2015].

James, R.G. et al., 2006. Odd-skipped related 1 is required for development of the metanephric kidney and regulates formation and differentiation of kidney precursor cells. *Development (Cambridge, England)*, 133(15), pp.2995–3004. Available at: http://www.ncbi.nlm.nih.gov/pubmed/16790474 [Accessed August 21, 2015].

James, R.G. & Schultheiss, T.M., 2005. Bmp signaling promotes intermediate mesoderm gene expression in a dose-dependent, cell-autonomous and translation-dependent manner. *Developmental biology*, 288(1), pp.113–25. Available at: http://www.ncbi.nlm.nih.gov/pubmed/16243309 [Accessed August 21, 2015].

Karner, C.M. et al., 2009. Wnt9b signaling regulates planar cell polarity and kidney tubule morphogenesis. *Nature genetics*, 41(7), pp.793–9. Available at: http://www.pubmedcentral.nih.gov/articlerender.fcgi?artid=2761080&tool=pmcentrez&rendertype=abstract [Accessed August 21, 2015].

Kerecuk, L., Schreuder, M.F. & Woolf, A.S., 2008. Renal tract malformations: perspectives for nephrologists. *Nature clinical practice. Nephrology*, 4(6), pp.312–25. Available at: http://www.ncbi.nlm.nih.gov/pubmed/18446149 [Accessed August 21, 2015].

Kobayashi, A. et al., 2005. Distinct and sequential tissue-specific activities of the LIM-class homeobox gene Lim1 for tubular morphogenesis during kidney development. *Development (Cambridge, England)*, 132(12), pp.2809–23. Available at: http://www.ncbi.nlm.nih.gov/pubmed/15930111 [Accessed August 21, 2015].

Kochhar, A. et al., 2007. Branchio-oto-renal syndrome. *American journal of medical genetics. Part A*, 143A(14), pp.1671–8. Available at: http://www.ncbi.nlm.nih.gov/pubmed/17238186 [Accessed August 21, 2015].

Lienkamp, S.S. et al., 2012. Vertebrate kidney tubules elongate using a planar cell polarity-dependent, rosette-based mechanism of convergent extension. *Nature genetics*, 44(12), pp.1382–7. Available at:

http://www.pubmedcentral.nih.gov/articlerender.fcgi?artid=4167614&tool=pmcentrez&rendertype=abstract [Accessed April 19, 2015].

Linton, J.M., Martin, G.R. & Reichardt, L.F., 2007. The ECM protein nephronectin promotes kidney development via integrin alpha8beta1-mediated stimulation of Gdnf expression. *Development (Cambridge, England)*, 134(13), pp.2501–9. Available at: http://www.pubmedcentral.nih.gov/articlerender.fcgi?artid=2757411&tool=pmcentrez&rendertype=abstract [Accessed August 21, 2015].

Livet, J. et al., 2007. Transgenic strategies for combinatorial expression of fluorescent proteins in the nervous system. *Nature*, 450(7166), pp.56–62. Available at: http://www.ncbi.nlm.nih.gov/pubmed/17972876 [Accessed July 10, 2014].

Luyten, A. et al., 2010. Aberrant regulation of planar cell polarity in polycystic kidney disease. *Journal of the American Society of Nephrology : JASN*, 21(9), pp.1521–32. Available at: http://www.pubmedcentral.nih.gov/articlerender.fcgi?artid=3013531&tool=pmcentrez&rendertype=abstract [Accessed August 21, 2015].

Maeshima, A. et al., 2006. Activin A is an endogenous inhibitor of ureteric bud outgrowth from the Wolffian duct. *Developmental biology*, 295(2), pp.473–85. Available at: http://www.ncbi.nlm.nih.gov/pubmed/16643884 [Accessed August 21, 2015].

Mathews, T.J. & MacDorman, M.F., 2013. Infant mortality statistics from the 2009 period linked birth/infant death data set. *National vital statistics reports : from the Centers for Disease Control and Prevention, National Center for Health Statistics, National Vital Statistics System*, 61(8), pp.1–27. Available at: http://www.ncbi.nlm.nih.gov/pubmed/24979974 [Accessed August 25, 2015].

Mauch, T.J. et al., 2000. Signals from trunk paraxial mesoderm induce pronephros formation in chick intermediate mesoderm. *Developmental biology*, 220(1), pp.62–75. Available at: http://www.ncbi.nlm.nih.gov/pubmed/10720431 [Accessed August 21, 2015].

McKenna, M.T. et al., 2005. Assessing the burden of disease in the United States using disability-adjusted life years. *American journal of preventive medicine*, 28(5), pp.415–23. Available at: http://www.ncbi.nlm.nih.gov/pubmed/15894144 [Accessed August 21, 2015].

McMahon, A.P. et al., 2008. GUDMAP: the genitourinary developmental molecular anatomy project. *Journal of the American Society of Nephrology : JASN*, 19(4), pp.667–71. Available at: http://www.ncbi.nlm.nih.gov/pubmed/18287559 [Accessed August 21, 2015].

Michos, O. et al., 2010. Kidney development in the absence of Gdnf and Spry1 requires Fgf10. *PLoS genetics*, 6(1), p.e1000809. Available at: http://www.pubmedcentral.nih.gov/articlerender.fcgi?artid=2797609&tool=p

mcentrez&rendertype=abstract [Accessed August 21, 2015].

Michos, O. et al., 2007. Reduction of BMP4 activity by gremlin 1 enables ureteric bud outgrowth and GDNF/WNT11 feedback signalling during kidney branching morphogenesis. *Development (Cambridge, England)*, 134(13), pp.2397–405. Available at: http://www.ncbi.nlm.nih.gov/pubmed/17522159 [Accessed August 21, 2015].

Miller, R.K. et al., 2011. Pronephric tubulogenesis requires Daam1-mediated planar cell polarity signaling. *Journal of the American Society of Nephrology : JASN*, 22(9), pp.1654–64. Available at: http://www.pubmedcentral.nih.gov/articlerender.fcgi?artid=3171937&tool=pmcentrez&rendertype=abstract [Accessed August 21, 2015].

Morris, A.R., Drawbridge, J. & Steinberg, M.S., 2003. Axolotl pronephric duct migration requires an epidermally derived, laminin 1-containing extracellular matrix and the integrin receptor alpha6beta1. *Development (Cambridge, England)*, 130(23), pp.5601–8. Available at: http://www.ncbi.nlm.nih.gov/pubmed/14522870 [Accessed October 6, 2015].

Narlis, M. et al., 2007. Pax2 and pax8 regulate branching morphogenesis and nephron differentiation in the developing kidney. *Journal of the American Society of Nephrology : JASN*, 18(4), pp.1121–9. Available at: http://jasn.asnjournals.org/content/18/4/1121.long [Accessed January 29, 2016].

Nie, X. et al., 2011. Six1 regulates Grem1 expression in the metanephric mesenchyme to initiate branching morphogenesis. *Developmental biology*, 352(1), pp.141–51. Available at: http://www.pubmedcentral.nih.gov/articlerender.fcgi?artid=3113441&tool=pmcentrez&rendertype=abstract [Accessed August 21, 2015].

Nishio, S. et al., 2010. Loss of oriented cell division does not initiate cyst formation. *Journal of the American Society of Nephrology : JASN*, 21(2), pp.295–302. Available at: http://www.pubmedcentral.nih.gov/articlerender.fcgi?artid=2834544&tool=pmcentrez&rendertype=abstract [Accessed August 21, 2015].

Nornes, H.O. et al., 1990. Spatially and temporally restricted expression of Pax2 during murine neurogenesis. *Development (Cambridge, England)*, 109(4), pp.797–809. Available at: http://www.ncbi.nlm.nih.gov/pubmed/1977575 [Accessed August 21, 2015].

Novak, A. et al., 2000. Z/EG, a double reporter mouse line that expresses enhanced green fluorescent protein upon Cre-mediated excision. *Genesis (New York, N.Y. : 2000)*, 28(3-4), pp.147–55. Available at: http://www.ncbi.nlm.nih.gov/pubmed/11105057 [Accessed July 31, 2015].

Obara-Ishihara, T. et al., 1999. The surface ectoderm is essential for nephric duct formation in intermediate mesoderm. *Development (Cambridge, England)*,

126(6), pp.1103–8. Available at: http://www.ncbi.nlm.nih.gov/pubmed/10021330 [Accessed August 25, 2015].

Overton, J., 1959. Mitotic Pattern in the Chick Pronephric Duct. *J Embryol Exp Morphol*, 7(3), pp.275–280. Available at: http://dev.biologists.org/content/7/3/275.short [Accessed October 31, 2015].

Pachnis, V., Mankoo, B. & Costantini, F., 1993. Expression of the c-ret proto-oncogene during mouse embryogenesis. *Development (Cambridge, England)*, 119(4), pp.1005–17. Available at: http://www.ncbi.nlm.nih.gov/pubmed/8306871 [Accessed August 21, 2015].

Pedersen, A., Skjong, C. & Shawlot, W., 2005. Lim 1 is required for nephric duct extension and ureteric bud morphogenesis. *Developmental biology*, 288(2), pp.571–81. Available at: http://www.ncbi.nlm.nih.gov/pubmed/16216236 [Accessed August 21, 2015].

Perälä, N. et al., 2011. Sema4C-Plexin B2 signalling modulates ureteric branching in developing kidney. *Differentiation; research in biological diversity*, 81(2), pp.81–91. Available at: http://www.ncbi.nlm.nih.gov/pubmed/21035938 [Accessed August 21, 2015].

Pfeffer, P.L. et al., 2002. The activation and maintenance of Pax2 expression at the mid-hindbrain boundary is controlled by separate enhancers. *Development (Cambridge, England)*, 129(2), pp.307–318. Available at: http://www.ncbi.nlm.nih.gov/pubmed/11807024 [Accessed August 21, 2015].

Poole, T.J. & Steinberg, M.S., 1981. Amphibian pronephric duct morphogenesis: segregation, cell rearrangement and directed migration of the Ambystoma duct rudiment. *Journal of embryology and experimental morphology*, 63, pp.1–16. Available at: http://www.ncbi.nlm.nih.gov/pubmed/7310283 [Accessed August 21, 2015].

Poole, T.J. & Steinberg, M.S., 1982. Evidence for the guidance of pronephric duct migration by a craniocaudally traveling adhesion gradient. *Developmental biology*, 92(1), pp.144–58. Available at: http://www.ncbi.nlm.nih.gov/pubmed/7049791 [Accessed August 21, 2015].

Püschel, A.W., Westerfield, M. & Dressler, G.R., 1992. Comparative analysis of Pax-2 protein distributions during neurulation in mice and zebrafish. *Mechanisms of development*, 38(3), pp.197–208. Available at: http://www.ncbi.nlm.nih.gov/pubmed/1457381 [Accessed August 21, 2015].

Qiao, J. et al., 1999. FGF-7 modulates ureteric bud growth and nephron number in the developing kidney. *Development (Cambridge, England)*, 126(3), pp.547–54. Available at: http://www.ncbi.nlm.nih.gov/pubmed/9876183 [Accessed August 21, 2015].

Renkema, K.Y. et al., 2011. Novel perspectives for investigating congenital anomalies of the kidney and urinary tract (CAKUT). *Nephrology, dialysis, transplantation : official publication of the European Dialysis and Transplant Association -*

European Renal Association, 26(12), pp.3843–51. Available at: http://www.ncbi.nlm.nih.gov/pubmed/22121240 [Accessed August 15, 2015].

Richardson, L. et al., 2014. EMAGE: Electronic Mouse Atlas of Gene Expression. *Methods in molecular biology (Clifton, N.J.)*, 1092, pp.61–79. Available at: http://www.ncbi.nlm.nih.gov/pubmed/24318814 [Accessed August 21, 2015].

Russo, C.A. & Elixhauser, A., Hospitalizations for Birth Defects, 2004. Available at: http://www.ncbi.nlm.nih.gov/books/NBK63495/ [Accessed August 25, 2015].

Saburi, S. et al., 2008. Loss of Fat4 disrupts PCP signaling and oriented cell division and leads to cystic kidney disease. *Nature genetics*, 40(8), pp.1010–5. Available at: http://www.ncbi.nlm.nih.gov/pubmed/18604206 [Accessed July 23, 2015].

Sajithlal, G. et al., 2005. Eya 1 acts as a critical regulator for specifying the metanephric mesenchyme. *Developmental biology*, 284(2), pp.323–36. Available at: http://www.pubmedcentral.nih.gov/articlerender.fcgi?artid=3876955&tool=pmcentrez&rendertype=abstract [Accessed August 21, 2015].

Sanna-Cherchi, S. et al., 2009. Renal outcome in patients with congenital anomalies of the kidney and urinary tract. *Kidney international*, 76(5), pp.528–33. Available at: http://www.ncbi.nlm.nih.gov/pubmed/19536081 [Accessed August 21, 2015].

Sanyanusin, P. et al., 1995. Mutation of PAX2 in two siblings with renal-coloboma syndrome. *Human molecular genetics*, 4(11), pp.2183–4. Available at: http://www.ncbi.nlm.nih.gov/pubmed/8589702 [Accessed January 29, 2016].

Shawlot, W. & Behringer, R.R., 1995. Requirement for Lim1 in head-organizer function. *Nature*, 374(6521), pp.425–30. Available at: http://www.ncbi.nlm.nih.gov/pubmed/7700351 [Accessed August 21, 2015].

Snippert, H.J. et al., 2010. Intestinal crypt homeostasis results from neutral competition between symmetrically dividing Lgr5 stem cells. *Cell*, 143(1), pp.134–44. Available at: http://www.cell.com/article/S0092867410010640/fulltext [Accessed April 1, 2015].

Song, R. & Yosypiv, I. V, 2011. Genetics of congenital anomalies of the kidney and urinary tract. *Pediatric nephrology (Berlin, Germany)*, 26(3), pp.353–64. Available at: http://www.ncbi.nlm.nih.gov/pubmed/20798957 [Accessed August 21, 2015].

STRONG, L.C. & HOLLANDER, W.F., 1949. HEREDITARY LOOP-TAIL IN THE HOUSE MOUSE: Accompanied by Imperforate Vagina and with Lethal Craniorachischisis When Homozygous. *J. Hered.*, 40(12), pp.329–334. Available at: http://jhered.oxfordjournals.org/content/40/12/329.extract [Accessed August 27, 2015].

Torban, E. et al., 2008. Genetic interaction between members of the Vangl family

causes neural tube defects in mice. *Proceedings of the National Academy of Sciences of the United States of America*, 105(9), pp.3449–54. Available at: http://www.pubmedcentral.nih.gov/articlerender.fcgi?artid=2265143&tool=pmcentrez&rendertype=abstract [Accessed August 21, 2015].

Torres, M. et al., 1995. Pax-2 controls multiple steps of urogenital development. *Development (Cambridge, England)*, 121(12), pp.4057–65. Available at: http://www.ncbi.nlm.nih.gov/pubmed/8575306 [Accessed August 21, 2015].

Tsang, T.E. et al., 2000. Lim1 activity is required for intermediate mesoderm differentiation in the mouse embryo. *Developmental biology*, 223(1), pp.77–90. Available at: http://www.ncbi.nlm.nih.gov/pubmed/10864462 [Accessed August 21, 2015].

Tufro, A. et al., Semaphorin3a inhibits ureteric bud branching morphogenesis. *Mechanisms of development*, 125(5-6), pp.558–68. Available at: http://www.pubmedcentral.nih.gov/articlerender.fcgi?artid=3992265&tool=pmcentrez&rendertype=abstract [Accessed August 21, 2015].

Uetani, N. & Bouchard, M., 2009. Plumbing in the embryo: developmental defects of the urinary tracts. *Clinical genetics*, 75(4), pp.307–17. Available at: http://www.ncbi.nlm.nih.gov/pubmed/19419410 [Accessed February 4, 2016].

Vize, P., Woolf, A. & Bard, J., 2003. *The kidney: from normal development to congenital disease*, Available at: https://books.google.ca/books?hl=en&lr=&id=ctOm-cPwo60C&oi=fnd&pg=PP1&ots=JF9TuK5hgW&sig=7SJJjfNm2rlyEn6HgwHrD2U3dbE [Accessed April 5, 2016].

Vize, P.D. et al., 1997. Model systems for the study of kidney development: use of the pronephros in the analysis of organ induction and patterning. *Developmental biology*, 188(2), pp.189–204. Available at: http://www.ncbi.nlm.nih.gov/pubmed/9268568 [Accessed August 21, 2015].

Weiss, A.-C. et al., 2014. Nephric duct insertion requires EphA4/EphA7 signaling from the pericloacal mesenchyme. *Development (Cambridge, England)*, 141(17), pp.3420–30. Available at: http://www.ncbi.nlm.nih.gov/pubmed/25139858 [Accessed August 27, 2015].

Wellik, D.M., Hawkes, P.J. & Capecchi, M.R., 2002. Hox11 paralogous genes are essential for metanephric kidney induction. *Genes & development*, 16(11), pp.1423–32. Available at: http://www.pubmedcentral.nih.gov/articlerender.fcgi?artid=186320&tool=pmcentrez&rendertype=abstract [Accessed August 21, 2015].

Wiesel, A. et al., 2005. Prenatal detection of congenital renal malformations by fetal ultrasonographic examination: an analysis of 709,030 births in 12 European countries. *European journal of medical genetics*, 48(2), pp.131–44. Available at: http://www.ncbi.nlm.nih.gov/pubmed/16053904 [Accessed August 6, 2015].

Wilm, B. et al., 2004. The forkhead genes, Foxc1 and Foxc2, regulate paraxial versus

intermediate mesoderm cell fate. *Developmental biology*, 271(1), pp.176–89. Available at: http://www.ncbi.nlm.nih.gov/pubmed/15196959 [Accessed August 21, 2015].

Xu, P.-X. et al., 2003. Six1 is required for the early organogenesis of mammalian kidney. *Development (Cambridge, England)*, 130(14), pp.3085–94. Available at: http://www.pubmedcentral.nih.gov/articlerender.fcgi?artid=3872112&tool=pmcentrez&rendertype=abstract [Accessed August 21, 2015].

Yates, L.L. et al., 2010. The planar cell polarity gene Vangl2 is required for mammalian kidney-branching morphogenesis and glomerular maturation. *Human molecular genetics*, 19(23), pp.4663–76. Available at: http://www.pubmedcentral.nih.gov/articlerender.fcgi?artid=2972698&tool=pmcentrez&rendertype=abstract [Accessed July 22, 2015].

Yu, J. et al., 2009. A Wnt7b-dependent pathway regulates the orientation of epithelial cell division and establishes the cortico-medullary axis of the mammalian kidney. *Development (Cambridge, England)*, 136(1), pp.161–71. Available at: http://www.pubmedcentral.nih.gov/articlerender.fcgi?artid=2685965&tool=pmcentrez&rendertype=abstract [Accessed August 21, 2015].

Yu, J., Carroll, T.J. & McMahon, A.P., 2002. Sonic hedgehog regulates proliferation and differentiation of mesenchymal cells in the mouse metanephric kidney. *Development (Cambridge, England)*, 129(22), pp.5301–5312. Available at: http://dev.biologists.org/content/129/22/5301.long [Accessed September 2, 2015].

Zhao, H. et al., 2004. Role of fibroblast growth factor receptors 1 and 2 in the ureteric bud. *Developmental biology*, 276(2), pp.403–15. Available at: http://www.pubmedcentral.nih.gov/articlerender.fcgi?artid=4131686&tool=pmcentrez&rendertype=abstract [Accessed August 27, 2015].

Supplementary Table 1. Primer sequences for guidance candidates

	Left Primer	Right Primer
anln	cagctcaaacaggaacgtga	cagaagtcaatggggtgctt
angpt1	aggcttggtttctcgtcaga	tctgcacagtctcgaaatgg
angpt2	gcatgtggtccttccaactt	tggtgtctctcagtgccttg
ar	ggaccatgttttacccatcg	tcgtttctgctggcacatag
BDNF	cagtggctggctctcttacc	tgctgccatgcataaaacat
Bmp1	ttcggcgataacaactaccc	tgctgtcgtagccatcaaag
Bmp2	tggaagtggcccatttagag	tgacgcttttctcgtttgtg
Bmp4	tgagcctttccagcaagttt	cttcccggtctcaggtatca
Bmp5	atcactgtgaccagcaacca	aagtacctcgcttgccttga
Bmp6	gaaggttggctggaatttga	acctcgctcaccttgaagaa
Bmp7	gaaaacagcagcagtgacca	ggtggcgttcatgtaggagt
Bmp8a	cacacagcatcccagagcta	ccacaatgaatggtgcagag
Bmp8b	gcagcctccctagctacctt	aaaccctgcacagatgaacc
Bmp10	ccctttgctggttgtgtttt	tcatgttcgacctcatctgc
Bmp15	attggagcgaaaatggtgag	aagtttccacatggcaggag
Efna1	cccacattacgaggacgact	gtgaagcgctggaatttctc
Efna5	tccagaggggtgactaccac	cttgaacccttggacgtgt
Egf	cccaggcaacgtatcaaagt	cccaggaaagcaatcacatt
Epgn	cgaagaagcagaggtgatcc	aatggcttgcttcagctcat
Epha1	gcaactatcatgggccagtt	gctgaccaggagctagttgg
epha2	aagacactgaaagcgggcta	tctagcgctccattctccat
ephb2	actatggcggctgtatgtcc	gcacatccacttcttcagca
ephb4	aatgtcaccactgaccgtga	tcaggaaacgaacactgctg
fgf1	ttcattcatgaggcctttcc	atgcagtacccctggagttg
Fgf2	agcggctctactgcaagaac	gccgtccatcttccttcata
fgf5	attagtggctgggctcaatg	agggggcagataaaaggaga
fgf6	ggccctgtgcataagaaaaa	caatcctgctgactcgacaa
fgf8	ccggacctaccagctctaca	actcggactctgcttccaaa
fgf9	gccagataggcattttggaa	catgagcgatgtgcagaagt
fgf10	ctggaaagcacttgggtcat	ggagacagaatgcacaagca
fgf12	gaccaaaaatttcccaagca	aaatggcacttcctgtggac
fgf13	cctcggaacatttcacacct	agtggtttgggcagaaaatg
fgf17	accagtacgtgagggaccag	tgctgccgaatgtatctgtc
fgf18	cctgcacttgcctgtgttta	cccaggacttgaatgtgctt
fgf20	gccgcatgtctctggataat	ccatctcagtgtggtgtggt
fgf22	gagatccgttctgtccgtgt	ttgtagccgttctcctcgat
fgfr1	atggttgaccgttctggaag	ggaagtcgctcttcttggtg
fgfr2	caccaactgcaccaatgaac	ggctgggtgagatccaagta
fgfr3	catccggcagacatacacac	ttcacttccacgtgcttcag

fgfr4	agcaccctactggacacacc	tgcctccaatacgattctcc
fgfrl1	tgtgaacacaacggtggact	gggcaacaccacaaacttct
gdf1	tccatctatgccaccgtgta	ctgacgtcatgcaggaagaa
gdf7	gatcatcgcgccattagact	gcggcatcgatgtagagaat
gdnf	cagcccctgctttctatctg	tatgttcagggcttccaagg
igf2	gagttcagagaggccaaacg	cctgctcaagaggaggtcac
igf1	actcaccaccctgtgacctc	ctcctggaaacccagaacaa
igf2r	tgggcttcccagaatatcag	ctccagagccaccttcagac
ihh	ccgaaccttcatcttggtgt	ccccgagaaacattggagta
inhbe	agcctgagacccccttatgt	ttggctttgaggaggctaaa
itga3	actacaggcggaacatcacc	tcatggcaatgacgatagga
itgb2	gtggtgcagctcatcaagaa	gccatgacctttacctggaa
itgb3	gctcattggccttgctactc	cccggtaggtgatattggtg
notch1	tgagactgccaaagtgttgc	gtgggagacagagtgggtgt
notch3	gggtcttgtctgctcaaagc	ggctgagccaagagaacaac
npy	tggactgaccctcgctctat	tgtctcagggctggatctct
nrg1	cagcaacccaagttctgtga	tgctgggttagtcctgctct
nrg3	gcatccagcacaaagtctga	gtgcttgataggctggcttc
nrg4	cagaccaagagtccagcaca	aataccagtttccgcacagg
nrp2	ttgtgtctggatcgcttctg	cagctgcatctccctttctc
ntn1	cccagagagtttccttgctg	tctccagctgttgacattgc
pigf	tttcattccgtccttcttcg	tttcaaagctcgcgttacct
plgf	aaccagccactcagaggaga	ttcctgagcgtcttgtcctt
plxna3	gctgttgatggcaagtctga	gaaggaggcactgacaaagc
plxnb1	agaggtggtggccatgatag	gcccatctgtaccgtgaact
plxnb2	aggggagcctctctacaagc	tcgatcccttcatcctgaac
prox1	ggagatggctgagaacaagc	agactttgaccaccgtgtcc
prox2	gtactcagaggagccgatgc	gaggtgaaggctggtttctg
ptn	gggtgggtgctaagaacaaa	gagggcagagagaagaagca
robo1	gccagcaaggaagaacagac	gcttcaattggccttagcag
sema3b	gctgtcttctccacctccag	acatgccaggtcttgggtag
sema3c	gagggctctacccttccatc	gccttcagcttgccatagtc
sema3e	ccatacaatgctgctggatg	cccggatataattggcacac
sema3f	agcttccagccacacctaga	ataaggggctctcggttgat
sema3g	cctgaagaggtggttttgga	gcactgccgtaagtctcaca
sema4a	ggcaccatgaacaacttcct	aagtcaaactcgctggctgt
sema4b	caaagtggctttgtgagcaa	tctggtccctgaggtggtag
sema4c	accagaccgaatgcttcaac	ttcccatcctcaaattctgc
sema4d	ttacggaggtatccgtggag	gttgaagaccaggccactgt
sema4f	agcagagatggacgacgttt	gaaggcacacacagcagaaa
sema4g	ccactcaagacccgatctgt	tagttgccactgtgctccag

sema5b	gtcacaggggaccactcact	ctgtgccaagagtcctgtga
sema6a	agtcctggagaagcagtgga	aggcacagactgcagaacct
slit1	ggacaatgaccacattgcag	accatctggtcgaaggtgac
slit2	cttgcctagagcgtcaaacc	ctttcggaatgaaacccaga
slit3	cttgtctccctgtccaccat	tggatgggaatctccttgag
shh	ctggccagatgttttctggt	ctcggctacgttgggaataa
spred1	cgcacagctgtttcactgat	tacaaatgctctgcgacagg
spred2	atggaccattaccaccctga	taggagtccgcgtcttctgt
spred3	ccaggtccttcattccttga	tgctgaaagactgtggcatc
spry1	ggcctattaggacggtctcc	ggccgtacactctccacatt
spry2	gggttaggggatttgtggtt	gcaatgtgggtctccaactt
spry3	ctacccccaatggacatcac	cattgcagacaaagcaagga
spry4	cagaattcttcctccccaca	gttcccaatgcctgttgact
tgfa2	aaggcatcttgggacaacac	gtccactggcctcttctctg
tgfb1	ttgcttcagctccacagaga	tggttgtagagggcaaggac
tgfb3	gaggctctggctttcatttg	ctccttgcattcacacctca
wnt1	cctacctccctccctctttg	aagaggtcacagcgcaaaat
wnt2	ggacctctgggttgttttca	tgtcatgccatttccaaaaa
wnt2b	cgaggtggcaaacatcctat	ctttgaaggctccactcctg
wnt3	gcgacttcctcaaggacaag	aaagttgggggagttctcgt
wnt4	acagctggagggctgactaa	tcttgacagtctggctggtg
wnt5a	ctggcaggactttctcaagg	gtctctcggctgcctatttg
wnt5b	ctctccgcctcacaaaagtc	ctctcccactggttgtggat
wnt7b	tccttgcagaactcgaggat	gcctgacacaagggacattt
wnt8a	atcacagggttggcctgtag	gagtaactgcgcaggaaagg
wnt8b	actcccgaaatggacaactg	ttacacgtgcgtttcatggt
wnt9b	agaacctgtcccctggtctt	tccagcactgaacaatgagc
wnt10	tgagagaggtggttggctct	gacctgtcctagggtgtgga
wnt10b	gggctcaggttcctacttcc	tgggctgtagtggaggagtt
wnt16	tgatgtccagtacggcatgt	caggttttcacagcacagga
vegfc	caaggcttttgaaggcaaag	tcccctgtcctggtattgag